Please cite this article in press as: Yadav et al., PGC1β Activates an Antiangiogenic Program to Repress Neoangiogenesis in Muscle Ischemia, Cell Reports (2014), http://dx.doi.org/10.1016/j.celrep.2014.06.040

Cell Reports
Article

PGC1β Activates an Antiangiogenic Program to Repress Neoangiogenesis in Muscle Ischemia

Vikas Yadav,[1] Antonios Matsakas,[1] Sabina Lorca,[1] and Vihang A. Narkar[1,2,3,*]
[1]Center for Metabolic and Degenerative Diseases, Brown Foundation Institute of Molecular Medicine for the Prevention of Human Diseases, University of Texas Medical School at Houston, 1825 Pressler Street, Houston, TX 77030, USA
[2]Department of Integrative Biology and Pharmacology, University of Texas Medical School at Houston, 6431 Fannin Street, Houston, TX 77030, USA
[3]Graduate School of Biomedical Sciences, University of Texas Medical School at Houston, 6767 Bertner Avenue, Houston, TX 77030, USA
*Correspondence: vihang.a.narkar@uth.tmc.edu
http://dx.doi.org/10.1016/j.celrep.2014.06.040

SUMMARY

Revascularization of ischemic skeletal muscle is governed by a balance between pro- and antiangiogenic factors in multiple cell types but particularly in myocytes and endothelial cells. Whereas the regulators of proangiogenic factors are well defined (e.g., hypoxia-inducible factor [HIF]), the transcriptional pathways encoding antiangiogenic factors remain unknown. We report that the transcriptional cofactor PGC1β drives an antiangiogenic gene program in muscle and endothelial cells. PGC1β transcriptionally represses proangiogenic genes (e.g., *Vegfc*, *Vegfd*, *Pdgfb*, *Angpt1*, *Angpt2*, *Fgf1*, and *Fgf2*) and induces antiangiogenic genes (e.g., *Thbs1*, *Thbs2*, *Angstat*, *Pedf*, and *Vash1*). Consequently, muscle-specific PGC1β overexpression impairs muscle revascularization in ischemia and PGC1β deletion enhances it. PGC1β overexpression or deletion in endothelial cells also blocks or stimulates angiogenesis, respectively. PGC1β stimulates the antiangiogenic genes partly by coactivating COUP-TFI. Furthermore, proangiogenic stimuli such as hypoxia, hypoxia-mimetic agents, and ischemia decrease PGC1β expression in a HIF-dependent manner. PGC1β is an antiangiogenic transcriptional switch that could be targeted for therapeutic angiogenesis.

INTRODUCTION

Skeletal muscle ischemia is a common problem in diseases such as diabetes, obesity, atherosclerosis, and aging, leading to peripheral vascular disease or critical limb ischemia (Baumgartner et al., 2005; Chi et al., 2011; Varu et al., 2010). Although inducing "therapeutic neoangiogenesis" to oppose ischemic muscle damage is a desirable treatment strategy, targeting individual angiogenic factors does not effectively revascularize infarcted muscles (Cao et al., 2005; Lekas et al., 2006; Simons and Ware, 2003; van Weel et al., 2008). Indeed, angiogenesis and vascularization constitute a complex process involving pro- and antiangiogenic factors that must be regulated in coordination, which makes it difficult to mimic the process with individual angiokines (Carmeliet and Jain, 2011). Proangiogenic factors such as vascular endothelial growth factor alpha (Vegfa) promote angiogenesis by triggering endothelial cell proliferation, migration, and differentiation (Carmeliet and Jain, 2011). On the other hand, antiangiogenic factors such as thrombospondin 1 (Thbs1) and Thbs2 limit angiogenesis by opposing Vegfa and endothelial cell proliferation and migration, as well as by inducing endothelial cell apoptosis (Lawler and Lawler, 2012). Uncovering the regulatory pathways that determine the balance between the pro- and antiangiogenic factors in muscle will yield candidates for therapeutic neoangiogenesis.

Various proangiogenic transcriptional pathways are defined in the skeletal muscle. A classic example is the master angiogenic regulator hypoxia-inducible factor (HIF) (Semenza, 2012), which when activated via adenoviral gene transfer or with synthetic agents induces neoangiogenesis in ischemic muscle (Milkiewicz et al., 2004; Pajusola et al., 2005; Sarkar et al., 2009). Recently, nuclear receptors and their coactivators have emerged as proangiogenic regulators in skeletal muscle. For example, the nuclear receptor cofactor peroxisome proliferator-activated receptor gamma coactivator 1 alpha (PGC1α) promotes muscle angiogenesis, possibly via estrogen-related receptor alpha (ERRα) or HIF (Arany et al., 2008; O'Hagan et al., 2009). Similarly, nuclear receptors, including ERRγ, peroxisome proliferator-activated receptor alpha (PPARα), and PPARδ, also stimulate ischemic neoangiogenesis by inducing stimulatory angiogenic factors such as Vegfa (Gaudel et al., 2008; Han et al., 2013; Matsakas et al., 2012b; Salehi et al., 2012). However, skeletal muscles also express a battery of inhibitory angiogenic factors that define the muscle vasculature, such as Thbs1, Thbs2, angiostatin (Angstat), vasohibin 1 (Vash1), and pigment epithelium-derived factor (PEDF) (Kivelä et al., 2006; Olfert and Birot, 2011). Surprisingly, how these angiostatic factors are transcriptionally regulated and affect ischemic muscle neoangiogenesis remains unclear.

In this study, we investigated the role of the transcriptional coactivator PGC1β in muscle neoangiogenesis. We report that PGC1β drives an antiangiogenic gene program in muscle and endothelial cells that involves repression of proangiogenic

Please cite this article in press as: Yadav et al., PGC1β Activates an Antiangiogenic Program to Repress Neoangiogenesis in Muscle Ischemia, Cell Reports (2014), http://dx.doi.org/10.1016/j.celrep.2014.06.040

factors and induction of antiangiogenic factors, which limits ischemic skeletal muscle revascularization. Our findings have implications for therapeutic angiogenesis in skeletal muscle. They may also be relevant for cardiac myopathies, retinopathy, and cancer, where neoangiogenesis is deregulated.

RESULTS

Regulation of the Antiangiogenic Gene Program by PGC1β in Muscle Cells

To obtain insight into the regulation of angiogenic factors by PGC1β, we made stable C2C12 cells overexpressing PGC1β or control vector. The PGC1β-overexpressing cells had higher levels of PGC1β mRNA (8- to 10-fold; Figure 1A, upper panel) and protein (Figure 1A, lower panel) compared with the control cells. A known gene target of PGC1β, cytochrome c (*Cycs*), was induced in PGC1β-overexpressing muscle cells, demonstrating the functionality of the overexpressed cofactor (Figure S1A). Another study reported that PGC1β induces Vegfa in skeletal muscles (Rowe et al., 2011). Accordingly, we found that Vegfa gene and protein expression was increased in C2C12 cells overexpressing PGC1β (Figures S1B and S1C). Although Vegfa is an important proangiogenic factor, there are several other pro- and antiangiogenic factors that collectively orchestrate the muscle angiogenic response (Kivelä et al., 2006; Olfert and Birot, 2011). Therefore, we subjected the control and PGC1β-overexpressing cells to an angiogenesis gene-expression analysis using a PCR-based gene array. The array profiles the expression of 84 genes known to regulate angiogenesis. The angiogenic profiling revealed that proangiogenic genes were predominantly repressed by PGC1β. At the same time, a battery of antiangiogenic genes were induced by PGC1β (Figure 1B; Table S1). To further elaborate these findings, we performed quantitative PCR (qPCR) for individual gene sets of the proangiogenic genes fibroblast growth factor 1 (*Fgf1*), *Fgf2*, platelet-derived growth factor beta (*Pdgfb*), angiopoietin 1 (*Angpt1*), *Angpt2*, *Vegfc*, and *Vegfd*, as well as the antiangiogenic genes *Angstat*, *Thbs1*, *Thbs2*, collagen 18a1 (the proteolytic fragment of which is antiangiokine Endostatin), *Vash1*, and *Pedf*. We found that PGC1β repressed proangiogenic genes (Figure 1C) and induced antiangiogenic genes (Figure 1D). These results demonstrate that PGC1β triggers a net antiangiogenic program in the muscle cells that results from the induction of antiangiogenic genes and repression of proangiogenic genes.

PGC1β Negatively Regulates Neoangiogenesis in Muscle Ischemia

The above results obtained with cultured cells indicate that PGC1β might signal muscle to preferentially secrete antiangiogenic factors to limit angiogenesis and muscle vascularization. To physiologically test the effect of activating PGC1β in muscle cells on the muscle vasculature, we generated transgenic (TG) mice selectively overexpressing PGC1β in skeletal muscles using the human alpha skeletal actin promoter (Muscat and Kedes, 1987). The structure of the transgene and the cloning strategy for transgene generation are described in Figures S2A and S2B. Briefly, the whole transgene was excised from the cloning vector by restriction digestion (Figure S2C), purified, and microinjected into oocytes to obtain mouse lines positive for the transgene (Figure S2D). From several TG lines obtained, the one that exhibited the lowest overexpression of PGC1β in the skeletal muscle was selected for further examination. The overexpression of PGC1β in the skeletal muscles at the gene/protein level was confirmed in the tibialis anterior (TA), soleus, quadriceps, and gastrocnemius (Figures S3A and S3B). It was previously reported that PGC1β induces genes linked to myofiber type (myosin heavy chain type IIx [MHC-IIx]), mitochondrial respiration (cytochrome c oxidase subunit Vb [*Cox5b*], ATP synthase, H^+ transporting, mitochondrial F1 complex, O subunit [*Atp5o*], *Cycs*, NADH dehydrogenase [ubiquinone] 1 alpha subcomplex 5 [*Ndufa5*]) and fatty acid oxidation (medium-chain acyl-CoA dehydrogenase [*Acadm*], carnitine palmitoyltransferase 1 [*Cpt1*], *Cpt2*, and cluster of differentiation 36 [*Cd36*]), and induces mitochondrial biogenesis in skeletal muscle (Arany et al., 2007). Similarly, in our muscle-specific PGC1β TG mice, we found that the aforementioned PGC1β target genes were induced in the TG muscles at both the transcript (Figures S3C–S3E) and protein (Figure S3F) levels, confirming an enhanced PGC1β signaling in the skeletal muscle of the TG mice. Additionally, PGC1β overexpression resulted in increased mitochondrial biogenesis and oxidative myofibers (Figures S3G and S3H), imparting red coloration to the TG mice (Figure S3I), as previously reported (Arany et al., 2007). Furthermore, we eliminated the possibility that PGC1β overexpression in the skeletal muscle might lead to muscle damage due to transgene overexpression by demonstrating healthy morphology and comparable serum creatine kinase levels (Figures S3J and S3K).

In these PGC1β TG mice and wild-type (WT) littermates, we next examined the expression of candidate pro- and antiangiogenic genes in the TA. We found that the expression of several proangiogenic genes (*Fgf2* and the *Vegfa* isoforms *Vegfa121*, *Vegfa165*, and *Vegfa189*) was predominantly downregulated in the TG compared with the WT TA muscles (Figure 2A). Vegfc and Ang2 did not change significantly. Note that the repression of proangiokines seemed to be more complete in adult murine muscle cells than in the cultured muscle cells, as even expression of the Vegfa isoforms was repressed in the former (Figures 2A and S1). On the other hand, the expression of antiangiogenic genes (*Thbs1*, *Thbs2*, *Pedf*, *Angstat*, *Vash1*, and Endostatin) was induced in the TG TA (Figure 2A). In correlation with gene expression, PGC1β repressed or induced pro- (FGF2) and antiangiogenic (THBS1, THBS2, ENDOSTATIN, and PEDF) factors, respectively, at the protein level (Figure 2B). Therefore, muscle PGC1β transcribes a net antiangiogenic signal that might in a paracrine fashion limit muscle neoangiogenesis in mice.

We tested this idea by first performing an angiogenesis tube-formation assay with TA homogenates obtained from WT and muscle-specific PGC1β TG mice. In this assay, tube formation in human umbilical vein endothelial cells (HUVECs) is used as a measure of angiogenesis. We found that whereas the control HUVECs treated with WT TA homogenates were able to differentiate into vessel-like structures, this effect was abolished in HUVECs treated with TG TA homogenates (Figure S4A). These findings confirm that PGC1β transcriptionally encodes antiangiogenic signaling in the skeletal muscle that can inhibit angiogenesis.

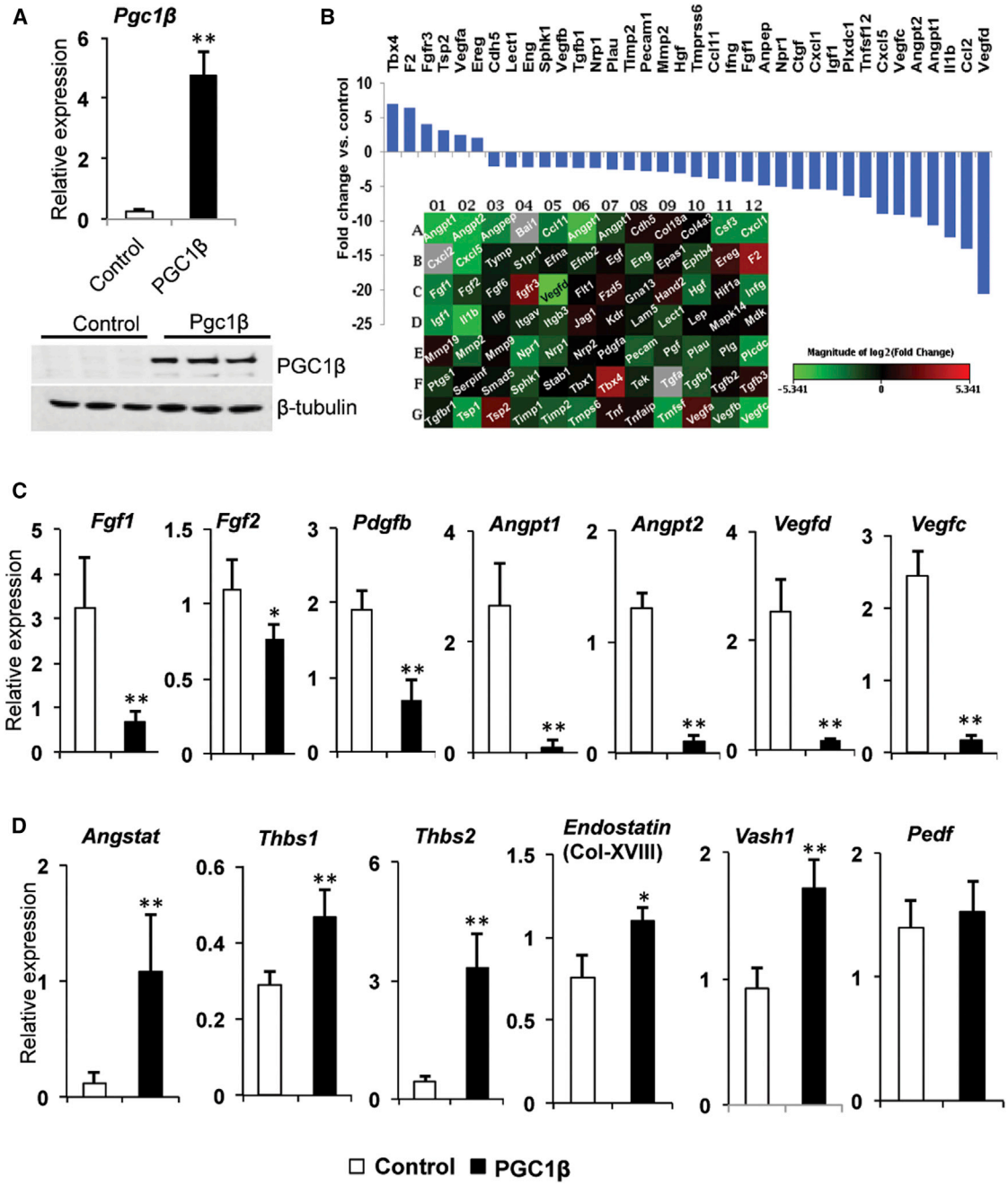

Figure 1. Regulation of Angiogenic Gene Expression by PGC1β

(A) PGC1β mRNA (top) and protein (bottom) expression in empty vector (control) and PGC1β-overexpressing C2C12 myotubes.

(B) Angiogenic PCR array data shown as fold change (≥2-fold and $p < 0.05$) for angiogenic gene expression in PGC1β-overexpressing C2C12 myotubes compared with control cells. Heatmap-based expression of all genes studied in the array, showing either repression (green) or induction (red).

(C and D) Relative mRNA expression of proangiogenic (C) and antiangiogenic (D) genes (n = 6, mean ± SD). *$p < 0.001$ and **$p < 0.000001$ (unpaired Student's t test).

See also Figure S1 and Table S1.

Because the aforementioned data pointed to an antiangiogenic role for PGC1β, we asked whether and how PGC1β might regulate ischemic muscle neoangiogenesis. We focused on a preclinical model for peripheral vascular disease, in which unilateral hindlimb ischemia is surgically induced in mice by ligating the femoral vessels in the left hindlimb (Matsakas et al., 2012b). The right hindlimb serves as a nonischemic control. The ischemic hindlimb undergoes spontaneous

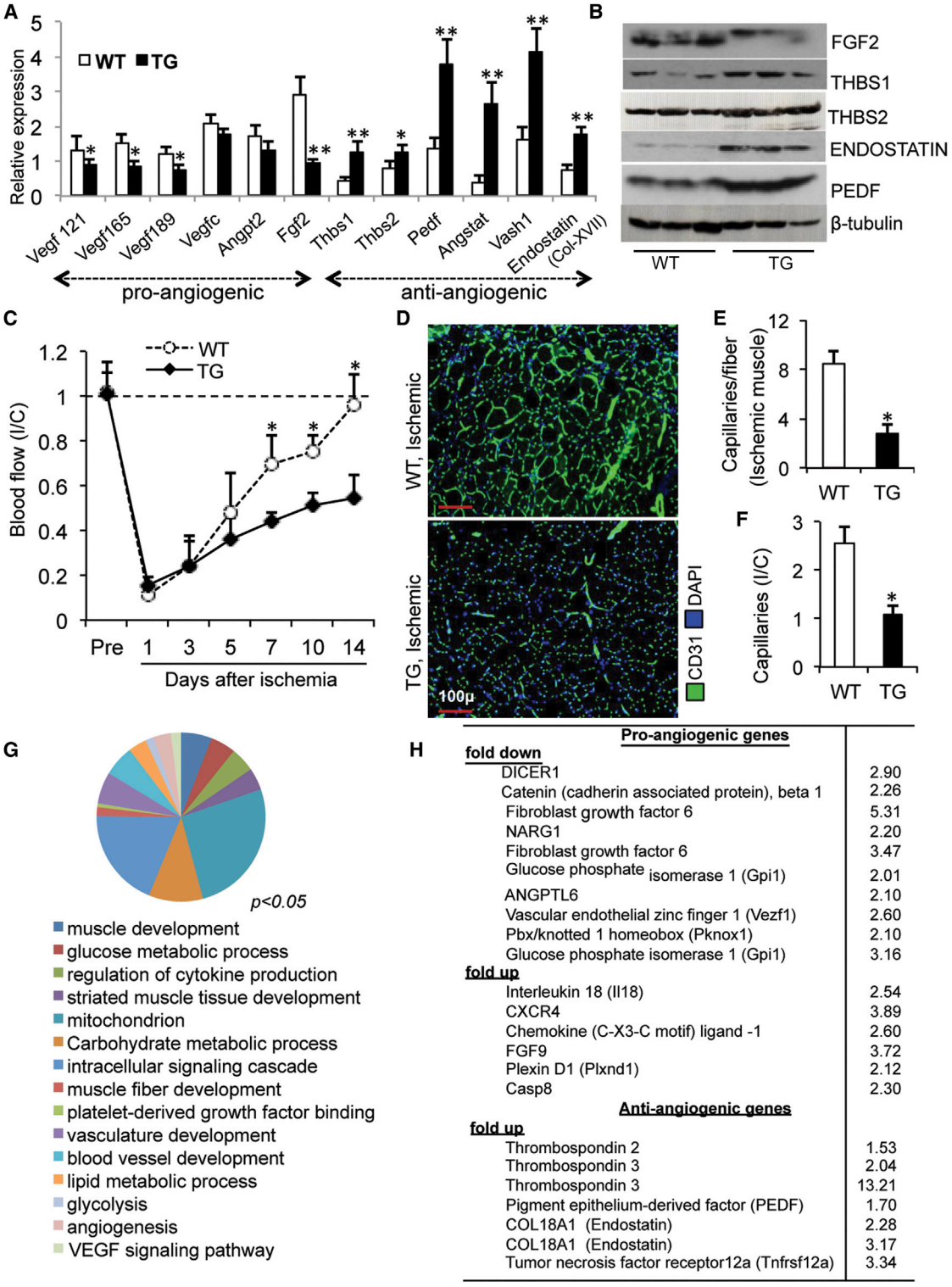

Figure 2. PGC1β Negatively Regulates Ischemic Revascularization

(A) Relative mRNA expression of pro- and antiangiogenic genes in TA from TG and WT mice (n = 5, mean ± SD). *p < 0.05 and **p < 0.001 (unpaired Student's t test).

(B) Representative western blots of FGF2, THBS1, THBS2, ENDOSTATIN, PEDF, and β-tubulin (as loading controls) in muscle extracts from GASTROC of TG and WT mice (n = 3).

(legend continued on next page)

revascularization over time and serves as a good model for exploring the regulation of neoangiogenesis (Matsakas et al., 2012b). To determine the role of PGC1β in ischemic revascularization or neoangiogenesis, we applied unilateral hindlimb ischemia to both muscle-specific PGC1β TG and WT littermate mice. Next, we measured skeletal muscle revascularization in these mice using laser-Doppler flowmetry. We found that whereas ischemic revascularization restored blood perfusion in the WT TA within 15 days, this process was impaired in the TG TA (Figure 2C). The baseline muscle blood flow was comparable between the WT and TG mice (WT = 6.14 ± 0.53 versus TG = 7.1 ± 0.77 [ml/min/100 g tissue]). Also, the two genotypes showed comparable muscle capillary staining (Figure S4B). Furthermore, the ischemic TG TA cryosections stained for the endothelial marker CD31 showed a dramatic decrease in endothelial-cell staining compared with the ischemic WT TA (Figure 2D; quantified in Figures 2E and 2F), demonstrating less capillarization in the PGC1β-overexpressing muscles. Therefore, PGC1β inhibits ischemic neoangiogenesis, but does not affect developmental skeletal muscle vascularization.

We investigated the comprehensive effect of PGC1β at the transcription level by performing a microarray analysis of TA muscles from WT and muscle-specific PGC1β TG mice. We found that PGC1β differentially regulated a total of 3,627 genes in skeletal muscles, of which 1,594 genes were upregulated and 2,033 were downregulated (Figure S5A). The Gene-Ontology-based classification of PGC1β-regulated genes in biological pathways is shown in Figure 2G, including gene sets linked to mitochondrial function (216), intracellular signaling (157), and carbohydrate/lipid metabolism (146). More relevantly, the pathway-based analysis confirmed that PGC1β downregulates proangiogenic genes and upregulates antiangiogenic genes, creating a net antiangiogenic signal (Figure 2H). Interestingly, genes linked to VEGF cellular signaling were also downregulated by PGC1β (Figure S5B), further supporting the antiangiogenic role of PGC1β.

To corroborate our findings from the PGC1β TG mice and examine the role of endogenous PGC1β in neoangiogenesis, we asked whether deletion of PGC1β expression actually accelerates ischemic skeletal muscle revascularization. For this purpose, we applied unilateral hindlimb ischemia to PGC1β$^{-/-}$ and WT littermate mice and measured the revascularization. We found that muscle revascularization in response to ischemic insult was enhanced in the PGC1β$^{-/-}$ mice compared with the WT mice (Figure 3A). The baseline muscle blood flow was comparable between the WT and PGC1β$^{-/-}$ mice (WT = 5.96 ± 0.75 versus PGC1β$^{-/-}$ = 6.07 ± 0.59 [ml/min/100 g tissue]). Whole-mount imaging of ischemic PGC1β$^{-/-}$ and WT muscles of mice perfused with microfil dye showed that PGC1β$^{-/-}$ muscles had enhanced vascularization compared with the WT muscles (Figures 3B [whole muscle] and 3C [microscopic image]). Notably, antiangiogenic genes such as *Thbs1*, *Thbs2*, and *Vash1* were downregulated in the PGC1β$^{-/-}$ compared with the WT muscles (Figures 3D and 3E). However, the expression of proangiogenic genes was unaffected by PGC1β deletion (data not shown), suggesting that the enhanced ischemic neoangiogenesis in the PGC1β$^{-/-}$ mice might be primarily due to the repression of antiangiogenic genes. Collectively, these findings indicate that PGC1β limits ischemic muscle neoangiogenesis, inactivation of which can enhance the process of revascularization.

PGC1β Signaling in Endothelial Cells

Our findings in skeletal muscle raised the possibility that endothelial PGC1β might also encode an antiangiogenic gene program. To test this, we used SVEC4-10 mouse endothelial cells for in vitro studies and mouse dorsal aortic ring explants for ex vivo endothelial cell sprouting assays. Overexpression of PGC1β in murine endothelial SVEC4-10 cells (Figure 4A) inhibited the expression of proangiogenic genes (*Angpt1*, *Angpt2*, *Fgf1*, *Fgf2*, *Vegfc*, and *Vegfd*; Figure 4B) but induced antiangiogenic genes (*Thbs1*, *Thbs2*, and *Vash1*; Figure 4C). Accordingly, PGC1β inhibited cell migration in these endothelial cells (Figure 4D; quantified in Fig. 4E), a classical angiogenic process. Next, we investigated the effect of PGC1β on endothelial cells in a commonly used aortic-ring angiogenesis assay. Lentiviral overexpression of PGC1β induced expression of *Thsb1* and *Thsb2* (Figure 4G), and thus blocked the aortic sprouting (Figure 4F). Conversely, sprouting was enhanced in aortic-ring explants from PGC1β$^{-/-}$ compared with WT mice (Figure 4H; quantified in Fig. 4I). Moreover, this effect was rescued by overexpression of PGC1β in the mutant aortic rings (Figures 4H and 4I). In support of this, antiangiogenic gene *Thbs1* expression was decreased in aortic explants from PGC1β$^{-/-}$ mice and restored by PGC1β overexpression (Figure 4J; for data regarding PGC1β expression in these groups, see Figures 4G and 4J). Therefore, the effect of PGC1β on angiogenic gene expression might be cell autonomous and the cofactor might repress angiogenesis particularly via effects in both the ischemic muscle and endothelial cells.

PGC1β Regulates Antiangiogenic Genes via COUP TF-I

PGC1β is a transcriptional cofactor and is known to interact with several transcription factors and nuclear receptors. Therefore,

(C) Postischemic blood-flow recovery (ischemic to contralateral ratio) in TG (filled diamonds) and WT (open circles) mice (n = 6, mean ± SD). **p < 0.001 represents statistically significant differences (two-way ANOVA and Bonferonni's multiple-comparison test).
(D) Representative TA cryosections from TG and WT mice 14 days postischemia immunostained for capillary structures (n = 3). Scale, 100 μm.
(E) Quantification of vascularization presented as capillaries/myofiber in ischemic TA from TG and WT muscles (n = 3, mean ± SD). *p < 0.01 (unpaired Student's t test).
(F) Ratio of CD31-positive cells (ischemic to contralateral) in TA from TG and WT (n = 3). *p < 0.01 (unpaired Student's t test).
(G) Pie chart showing the major cellular pathways transcriptionally regulated by PGC1β (>2-fold) in the microarray analysis of TA from TG and WT mice (n = 3; p < 0.05).
(H) Up- or downregulated pro- and antiangiogenic genes from the microarray analysis (p < 0.05).
See also Figures S2–S5.

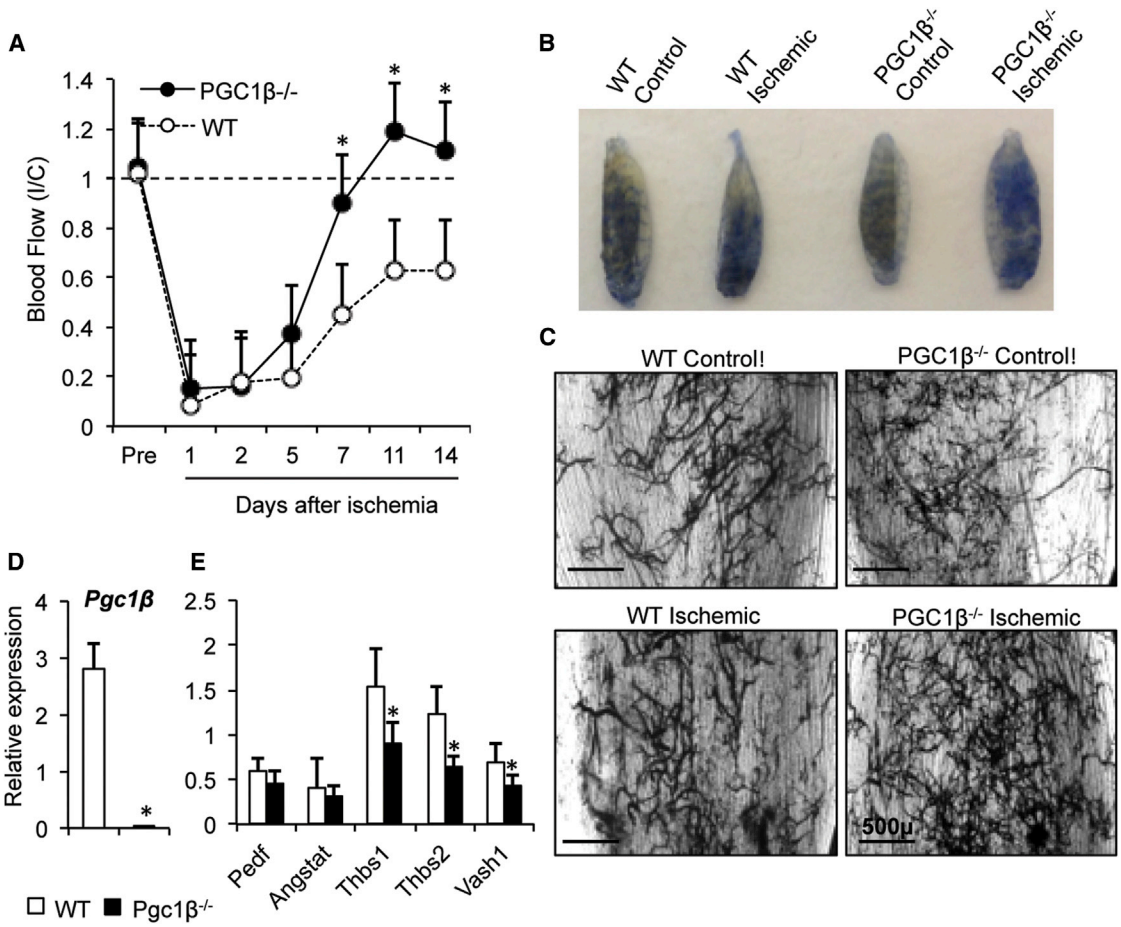

Figure 3. Loss of PGC1β Enhances Ischemic Revascularization

(A) Postischemic perfusion in PGC1β$^{-/-}$ and WT littermate mice (n = 6, mean ± SD). *p < 0.01 (two-way ANOVA and Bonferonni's multiple-comparison test).

(B) Representative images of TA muscles perfused with microfil dye to detect intact vasculature in PGC1β$^{-/-}$ and WT mice.

(C) Whole-mount image of microfilm perfused TA from PGC1β$^{-/-}$ and WT mice (n = 3). Scale, 500 μm.

(D and E) Relative mRNA expression of PGC1β (D) and antiangiogenic (E) genes in TA from PGC1β$^{-/-}$ and WT mice (n = 5, mean ± SD). *p < 0.05 (unpaired Student's t test).

PGC1β might regulate angiogenic genes by activating one or more transcriptional factors on different genes. To reveal the mechanism by which PGC1β regulates the antiangiogenic gene program, we examined the promoters and first intronic regions of the potent antiangiogenic factors Thbs1 and Thbs2. We targeted these two genes to focus more on the regulation of antiangiogenic genes by PGC1β. We found that both of these genes possess a consensus sequence for COUP-TF1 binding (5′-(A/G)G(G/T)TCA-3′) (Figures 5A and 5B). To gain further insight, we performed chromatin immunoprecipitation (ChIP) on sheared chromatin from C2C12 myotubes expressing histidine-tagged PGC1β (PGC1β-HIS) using an antihistidine antibody. We found PGC1β enrichment at the COUP TF-I binding sites in the Thbs1 (site −2,030) and Thbs2 (site −1,064) promoter regions (Figures 5C and 5D). Next, we tested whether PGC1β regulates *Thbs1* and *Thbs2* by activating COUP TF-I. In transient transfection experiments, PGC1β overexpression in C2C12 cells induced both *Thbs1* and *Thbs2*, an effect that was further enhanced in the presence of COUP-TFI (Figures 5E and 5F). To further support our findings, 2.7 kb of human THBS1 (hTHBS1) and 2.85 kb of mouse Thsb2 (mThsb2) genomic DNA fragments encompassing the COUP-TF1 binding sites were cloned 5′ to a luciferase reporter gene. In 293T cells, cotransfection of PGC1β with COUP-TF1 activated both THBS1 and THBS2 promoter activities compared to controls, whereas cotransfection of PGC1β with COUP-TFII did not activate either promoter. In reporter gene assays, both the Thbs1 and Thbs2 promoters were synergistically activated by PGC1β and COUP TF-I (Figures 5G and 5H). Interestingly, we also found that COUP-TFI (but not COUP-TFII) gene and protein expression was induced by PGC1β in the skeletal muscles isolated from PGC1β TG mice compared to the WT mice (Figures 5I–5K). PGC1β overexpression similarly induced COUP-TFI expression in C2C12 cells (Figure S6). Therefore, PGC1β might stimulate some of the antiangiogenic genes by inducing as well as coactivating the orphan nuclear receptor COUP-TFI.

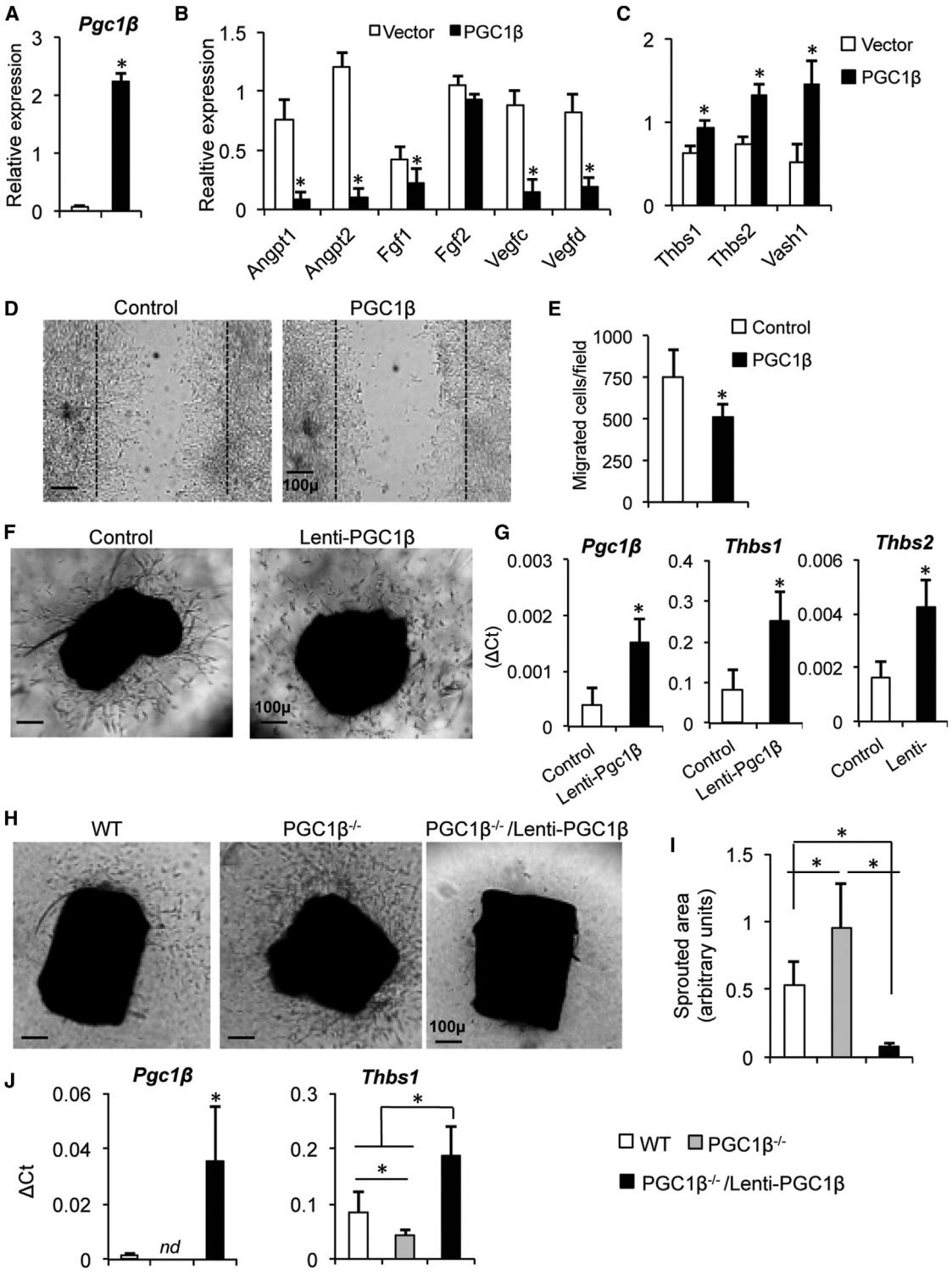

Figure 4. PGC1β Negatively Regulates Angiogenesis in Endothelial Cells

(A) PGC1β mRNA expression in empty vector (control) and PGC1β-overexpressing SVEC4-10 endothelial cells.

(B and C) Relative mRNA expression of pro- and antiangiogenic genes in SVEC4-10 cells overexpressing PGC1β and compared with control cells (n = 6, mean ± SD). *p < 0.01 (unpaired Student's t test).

(D and E) PGC1β-overexpressing SVEC4-10 cells are hypomigratory in a scratch assay.

(F) Dorsal aortic-ring assay in aortic explants infected with either PGC1β (lenti-PGC1β) or empty vector (control) lentivirus (n = 10).

(legend continued on next page)

Please cite this article in press as: Yadav et al., PGC1β Activates an Antiangiogenic Program to Repress Neoangiogenesis in Muscle Ischemia, Cell Reports (2014), http://dx.doi.org/10.1016/j.celrep.2014.06.040

Hypoxia Represses PGC1β Expression

Hypoxia is a hallmark of ischemic diseases and activates a proangiogenic gene program to promote revascularization (Semenza, 2009). Because our results showed that PGC1β is an antiangiogenic regulator, we rationalized that hypoxia would downregulate PGC1β. Indeed, PGC1β gene expression was reduced in C2C12 muscle cells subjected to 6 hr of hypoxia compared to those in normoxia (Figure 6A). The same hypoxic conditions that repressed PGC1β robustly induced hallmark hypoxia-stimulated proangiogenic factors (e.g., *Vegfa*, *Vegfd*, *Nos2*, and *Fgf1*) in the C2C12 cells (Figure 6B). Additionally, we investigated whether the hypoxia-mimetic drug dimethyloxaloylglycine (DMOG) could also repress PGC1β expression. Treatment of C2C12 cells with DMOG (1 mM) repressed PGC1β expression and simultaneously increased *Vegfa*, *Vegfd*, *Nos2*, and *Fgf1* expression (Figures 6C and 6D). Similar to what was observed for gene expression, hypoxia also reduced PGC1β protein expression under conditions that stimulated the expression of proangiogenic factors (Figure 6E). Similar to the case with hypoxia, PGC1β expression was also inhibited 4 days after ischemia in the skeletal muscle (Figure 6F). Interestingly, hypoxia also repressed PGC1β expression in endothelial cells (HUVECs and SVEC4-10; Figures S7A and S7B). Therefore, our results unequivocally show that PGC1β expression is inhibited by hypoxia, a hypoxia-mimetic drug, and ischemia, which is congruous with the antiangiogenic role of PGC1β.

Hypoxic Repression of PGC1β Is Mediated by HIF Signaling

HIF is a central hypoxic regulator that stimulates a robust proangiogenic gene program (Semenza, 2009, 2012). Therefore, we hypothesized that HIF itself mediates hypoxic repression of PGC1β. To test this hypothesis, we investigated whether the hypoxic repression of PGC1β is lost in cells devoid of HIF signaling. To do so, we used cells lacking HIF1B (also known as aryl hydrocarbon receptor nuclear translocator [ARNT]; $ARNT^-$ cells, ATCC #CRL-2717) as well as control cells that express HIF1B/ARNT ($ARNT^+$ cells, ATCC# CRL-2712) (Wood et al., 1996). HIF1B/ARNT is an obligatory heterodimeric partner in the HIF signaling complex, without which the cells are devoid of HIF signaling (Semenza, 2012; Wood et al., 1996). We subjected both the $ARNT^+$ and $ARNT^-$ cells to hypoxia for 6 hr and then measured the gene expression of PGC1β as well as the HIF target genes *Vegfa* and *Nos2*. We found that, similar to what was observed in muscle cells, hypoxia repressed PGC1β expression in the control $ARNT^+$ cells. Not only was this effect lost in $ARNT^-$ cells, but also PGC1β expression was surprisingly induced under hypoxic conditions in these cells (Figure 7A). We showed that expression of the HIF target genes *Vegfa* and *Nos2* was induced in $ARNT^+$ cells by hypoxia, but this effect was lost in $ARNT^-$ cells, confirming the lack of HIF signaling (Figure 7B).

We further explored the involvement of HIF in hypoxic repression of PGC1β in muscle cells. We overexpressed constitutively active HIF1A (HIF1A-CA) or control vector in C2C12 cells and subjected the infected cells to 6 hr of hypoxia or normoxia. In control cells, PGC1β was repressed by hypoxia. PGC1β gene expression was repressed by HIF1A-CA even in normoxia. The hypoxic repression of PGC1β was further exaggerated in muscle cells expressing HIF1A-CA (Figure 7C). At the protein level, HIF1A-CA repressed PGC1β expression similarly to hypoxic repression of the cofactor (Figure 7D; quantified in Figure 7E).

Next, we determined whether HIF represses PGC1β transcription by direct promoter occupancy on the *Pgc1β* gene. For this purpose, we searched the *Pgc1β* gene promoter and first intronic region for the presence of the HIF response element (HRE) consensus sequence ((A/G)CGTG(C/G)). We found at least one binding site in the promoter region and six sites in the first intron (Figure 7F). Accordingly, we performed ChIP for HIF occupancy on these HRE sites in the endogenous *Pgc1β* gene. ChIP was performed with C2C12 cells using HA-tagged HIF1A under hypoxia and normoxia. Chromatin was precipitated with anti-HA followed by PCR and qPCR using primers flanking the HRE sites. We observed that HIF1A occupied the *Pgc1β* gene at the +1,005 bp position in the first intron with enhanced occupancy under hypoxic conditions (Figures 7G and 7H). As a positive control, we show Vegfa gene occupancy by HIF1A under normoxia and hypoxia. To determine whether HIF1A regulates the PGC1β promoter activity, 500 bp and 450 bp fragments of DNA surrounded by HIF1A-binding sites from the PGC1β first intron corresponding to positions +1,005 and +1,929, respectively, were cloned 5′ to a luciferase reporter gene. First, the 293T cells were cotransfected with the PGC1β luciferase construct (+1,005) and plasmids encoding for HIF1A or HIF1A-CA. Whereas HIF1A-CA was sufficient to suppress the PGC1β promoter activity under both normoxia and hypoxia, HIF1A blocked the promoter activity only under hypoxic conditions (Figure 7I). In contrast, the PGC1β luciferase construct with the +1,929 HIF1A site was not repressed by HIF1A in either normoxia or hypoxia (Figure 7J).

Collectively, our findings demonstrate that hypoxia (a proangiogenic stimuli) represses PGC1β in a HIF-dependent fashion, and provide a molecular basis to explain how pro- and antiangiogenic genes might be balanced in hypoxia or ischemia to promote neoangiogenesis (Figure 7K).

DISCUSSION

Loss of skeletal muscle vasculature leading to limb amputation is a common complication in metabolic and cardiovascular diseases. Although muscle angiogenesis is governed by a balance between pro- and antiangiogenic factors, most studies have focused on the molecular regulators of proangiogenic factors. How the antiangiogenic program is encoded is poorly defined.

(G) mRNA expression of PGC1β, Thbs1, and Thbs2 in mouse aortic explants at day 7 (n = 4, mean ± SD). *p < 0.01 (unpaired Student's t test).
(H) Aortic-ring assay in WT, $PGC1\beta^{-/-}$, and $PGC1\beta^{-/-}$-infected $PGC1\beta^{-/-}$ aortic explants (n = 7).
(I) Quantification of the sprouted area from the aortic rings shown in (H).
(J) mRNA expression of Pgc1β and Thbs1 in mouse aortic explants at day 7 (n = 3, mean ± SD). *p < 0.05 (unpaired Student's t test); nd, not detectable (Ct ≥ 35).
Where indicated, scale bar represents 100 μm.

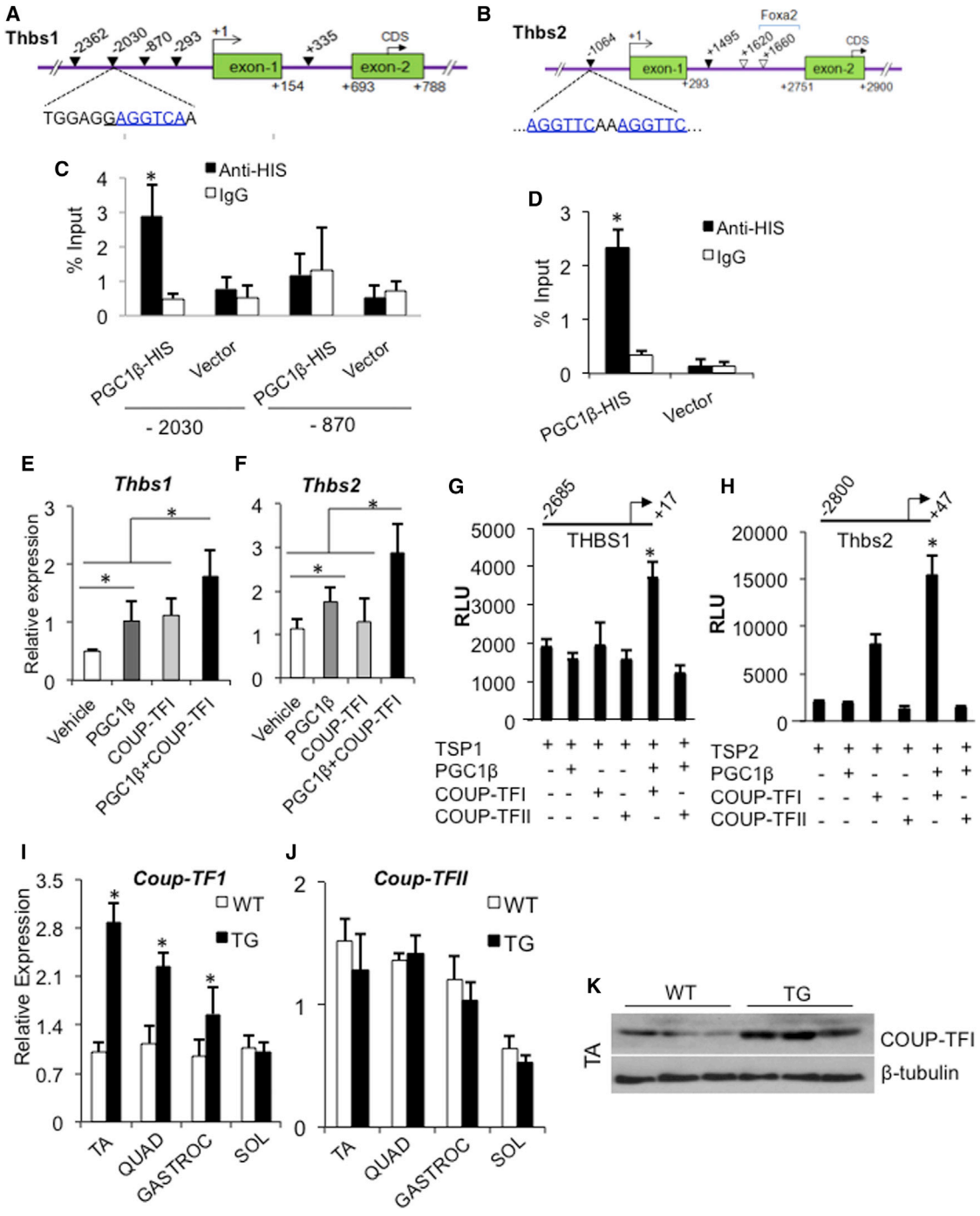

Figure 5. PGC1β Regulates the Expression of Thbs1 and Thbs2 by Coactivating COUP-TFI

(A and B) COUP-TF responsive elements (COUP-RE) in the promoter and first intron of THBS1 (A) and THBS2 (B) genes. Underlined nucleotides show the direct repeat (DR) of the COUP-TF binding sequence (ATTGGC).

(C and D) ChIP qPCR for the occupancy of HIS-tagged PGC1β at COUP-TF binding regions on the THBS1 promoter (−2,030 and −870 sites) and THBS2 gene promoter at the −1,064 site (n = 3, mean ± SD). *p < 0.01 (unpaired Student's t test).

(E and F) Cotransfection of PGC1β and COUP-TFI is able to induce both Thbs1 and Thbs2 in C2C12 myotubes (n = 4, mean ± SD). **p < 0.05 (unpaired Student's t test).

(G and H) Reporter assays for mouse THBS2 (mTHBS2) or human THBS1 (hTHBS1) promoter activation by PGC1β, COUP-TFI, COUP-TFII, PGC1β + COUP-TFI, and PGC1β + COUP-TFII (n = 6, mean ± SD). **p < 0.001 (unpaired Student's t test).

(legend continued on next page)

Please cite this article in press as: Yadav et al., PGC1β Activates an Antiangiogenic Program to Repress Neoangiogenesis in Muscle Ischemia, Cell Reports (2014), http://dx.doi.org/10.1016/j.celrep.2014.06.040

We show that the nuclear receptor coactivator PGC1β activates an antiangiogenic program in both muscle and endothelial cells by inhibiting proangiogenic genes and stimulating antiangiogenic genes. Consequently, PGC1β delays revascularization of the skeletal muscle in ischemia. The PGC1β antiangiogenic gene program is partly dependent on activation of the orphan nuclear receptor COUP-TFI. Interestingly, PGC1β is downregulated in response to ischemia, hypoxia, or a hypoxia-mimetic drug in a HIF1A-dependent fashion. Therefore, PGC1β is a HIF1A-regulated antiangiogenic factor that could be targeted for therapeutic angiogenesis.

The previously reported proangiogenic function of PGC1α in controlling muscle vasculature by stimulating Vegfa (Arany et al., 2008; Chinsomboon et al., 2009) prompted us to ask whether PGC1β also regulates angiogenesis. We found that in contrast to PGC1α, PGC1β represses proangiogenic genes in muscle cells, most of which encode secretory angiokines that promote angiogenesis, such as *Fgf1*, *Fgf2*, *Vegfc*, and *Vegfd*. In addition, PGC1β transcriptionally stimulates the expression of antiangiogenic secretory factors that repress angiogenesis, such as *Thbs1*, *Thbs2*, *Angstat*, and *Vash1*. Accordingly, muscle lysates from TG muscles overexpressing PGC1β blocked tube formation in HUVECs, demonstrating a net antiangiogenic signal emanating from PGC1β-activated muscles. It was recently shown that PGC1β overexpression in muscle cells induced Vegfa expression (Rowe et al., 2011). However, a comprehensive profiling of angiogenic factors was not performed in that study. We observed a similar induction of Vegfa in C2C12 muscle cells overexpressing PGC1β. However, in our studies, overexpression of PGC1β in rodent muscles neither induced Vegfa isoforms nor changed the basal vasculature or blood flow in the skeletal muscles. A global gene-expression analysis generally revealed a repression of proangiogenic genes and a stimulation of antiangiogenic genes by PGC1β in the skeletal muscles. Indeed, overexpression of PGC1β in the skeletal muscles inhibited revascularization of the muscles in response to ischemic attack. The antiangiogenic role of PGC1β, specifically the endogenously expressed coactivator, was further confirmed by our observation that ischemic revascularization of the skeletal muscle was enhanced in PGC1β$^{-/-}$ compared with WT mice. Therefore, PGC1β drives a net antiangiogenic gene program that involves inhibition of proangiogenic genes and stimulation of antiangiogenic genes, and blocks neoangiogenesis and revascularization in the skeletal muscles.

We found that the antiangiogenic gene effects of PGC1β are cell autonomous. Similarly to muscle cells, PGC1β activates an antiangiogenic program in endothelial cells that leads to blockade of angiogenic phenomena, as revealed by in vitro angiogenesis assays for endothelial cell migration and dorsal aortic-ring sprouting. In contrast, the angiogenic effects of PGC1α seem to be cell-type specific. Whereas PGC1α activates angiogenesis in muscle through paracrine secretion of proangiogenic factors such as Vegfa (Arany et al., 2008), it inhibits angiogenesis by activating notch signaling and blunting the effects of proangiogenic factors in endothelial cells (Sawada et al., 2014). Activation of notch signaling in endothelial cells is responsible for limiting angiogenesis and maintaining the cells in quiescence (Guarani et al., 2011). Whether PGC1β activates notch signaling in endothelial cells is unknown and will be interesting to examine in the future. Likewise, the regulation of smooth muscle cells by PGCs and how this regulation contributes to vascularization will be crucial to investigate.

PGC1β orchestrates gene expression by activating multiple transcriptional factors or nuclear receptors (Finck and Kelly, 2006). While it can be envisioned that a similar mechanism is at play in the regulation of angiogenesis by PGC1β, we focused on the regulation of the potent antiangiogenic factors Thbs1 and Thsb2 to identify at least one transcriptional factor involved in PGC1β effects. We chose to focus on these antiangiogenic genes because of the need to improve our understanding of how antiangiogenic factors are regulated in the muscle. We observed that both of these genes have orphan nuclear receptor COUP-TFI binding sites in the promoter and first intronic regions. We found that PGC1β-dependent regulation of both of these genes was enhanced in the presence of the orphan nuclear receptor COUP-TFI, and PGC1β binds at the COUP-TFI binding site in the promoters of Thbs1 and Thbs2. Interestingly, COUP-TFI was itself induced by PGC1β overexpression in the skeletal muscles, potentially suggesting a dual effect on COUP-TF1 in regulating antiangiogenic genes. Interestingly, a related orphan nuclear receptor, COUP-TFII, is known to regulate angiogenesis (Pereira et al., 1999; Qin et al., 2010). However, PGC1β neither increased COUP-TFII expression nor regulated Thbs1 and Thbs2 through COUP-TFII. Although not much is known regarding how COUP-TF1 regulates angiogenesis, our results preliminarily suggest that COUP-TFI might be a PGC1β-activated antiangiogenic factor.

In concert with the antiangiogenic role of PGC1β, we found that PGC1β is downregulated by hypoxia, the hypoxia-mimetic drug DMOG, and ischemia. Since all of these conditions activate HIF1A, we investigated whether HIF1A is responsible for blocking PGC1β expression. The inhibition of PGC1β expression by hypoxia is lost in cells lacking HIF1A signaling, suggesting a direct regulation of the coactivator expression by HIF1A. Indeed, HIF1A inhibits PGC1β gene expression by directly binding at the first intronic site in the PGC1β gene. Notably, expression of PGC1β is decreased in VHL-dependent renal carcinoma cells, in which HIF1 activity is high (Zhang et al., 2007). In these cells, PGC1β expression is controlled by C-MYC, which in turn is downregulated or degraded by HIF1A. Direct regulation of PGC1β by HIF1 was not examined in this study. Nevertheless, downregulation of PGC1β is a component of the hypoxic or HIF1A activation response, which is in agreement with the antiangiogenic role of the coactivator.

Why PGC1β-driven antiangiogenic genes do not affect the vascular supply in normoxic muscle is not clear. In terms of fiber

(I and J) Relative expression of COUP-TFI (I) and COUP-TFII (J) in various muscle beds from TG and WT mice (n = 5, mean ± SD). **$p < 0.01$ (unpaired Student's t test).

(K) Representative western blots for of COUP-TFI and β-tubulin (as loading control) in TA from TG and WT mice (n = 3).

See also Figure S6.

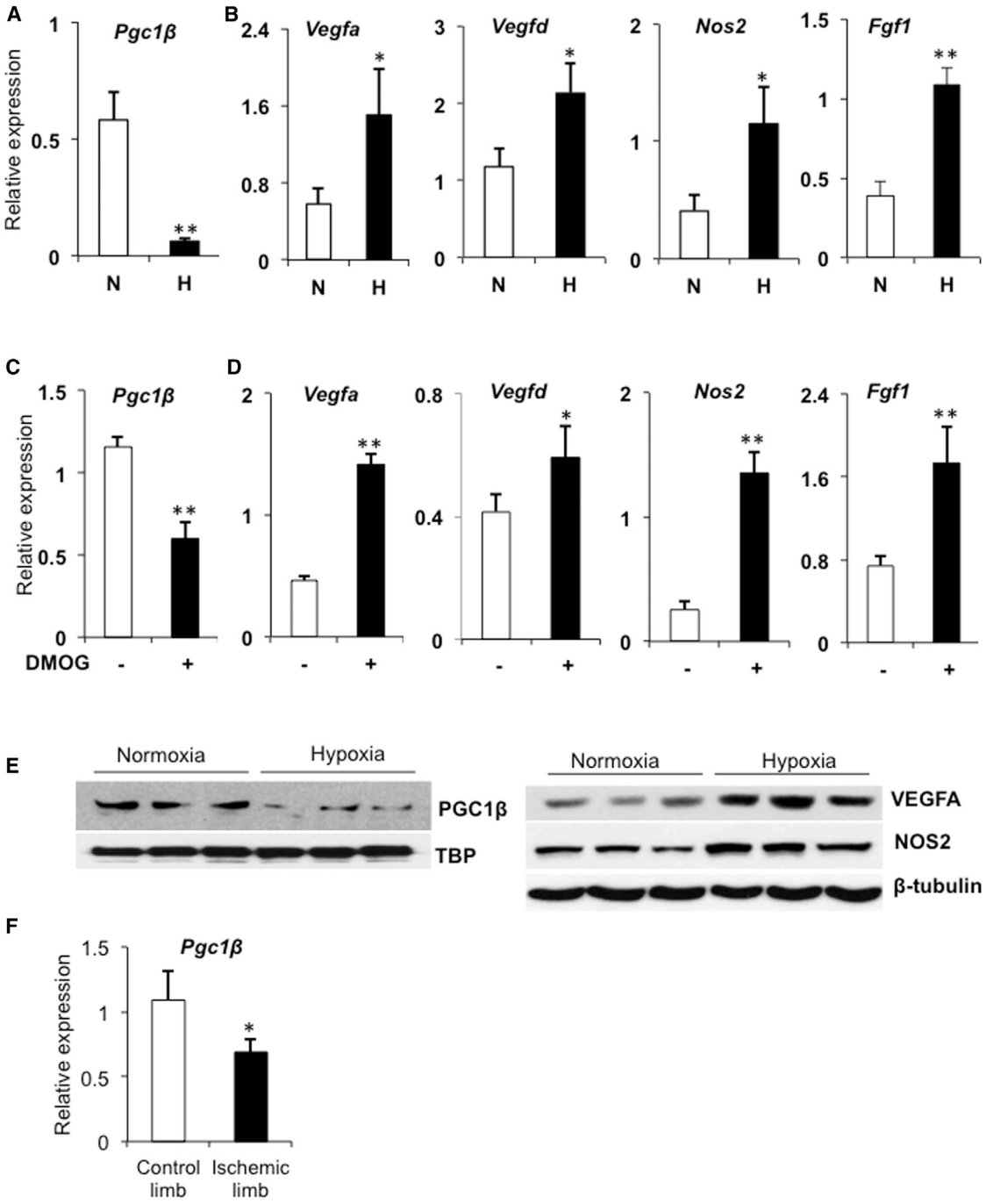

Figure 6. Regulation of PGC1β by Hypoxia

(A and B) PGC1β (A) and proangiogenic (B) gene expression in C2C12 myotubes subjected to hypoxia (H) or normoxia (N) for 6 hr (n = 6).

(C and D) PGC1β (C) and proangiogenic (D) gene expression in C2C12 myotubes treated for 24 hr with the hypoxia-mimetic drug DMOG (1 mM; n = 5). In (A)–(D), data are presented as mean ± SD. *p < 0.01, **p < 0.0001 (unpaired Student's t test).

(E) Representative western blots of PGC1β and TBP (as loading controls) in nuclear extracts and VEGFA, NOS2, and β-Tubulin (as loading controls) in cytoplasmic extracts from C2C12 myotubes subjected to either normoxia or hypoxia for 6 hr.

(F) mRNA level of PGC1β in control and 4-day postischemic quadriceps (n = 4, mean ± SD). *p < 0.05 (unpaired Student's t test).

See also Figures S7A and S7B.

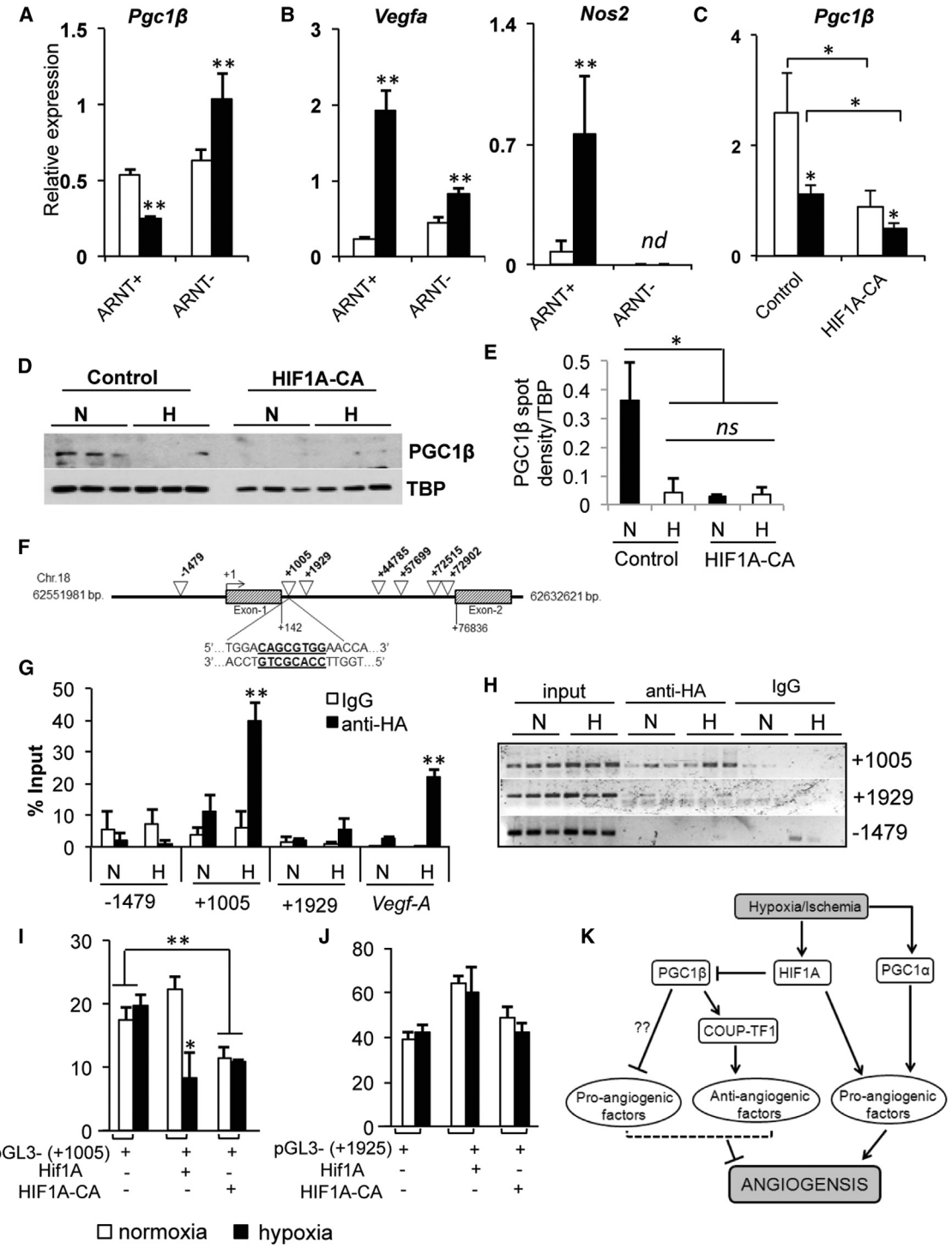

Figure 7. Hypoxic Repression of PGC1β Is Mediated by HIF1A

(A and B) Expression of PGC1β (A) and the HIF1 target genes Vegfa and NOS2 (B) in ARNT^{+} and ARNT^{-} cells subjected to normoxia (open bar) or hypoxia (closed bar) for 6 hr (n = 5, mean ± SD). *p < 0.01 and **p < 0.0001 (unpaired Student's t test); nd, not detectable (Ct ≥ 35).

(C) Expression of PGC1β in control or constitutively active human HIF1A (HIF1A-CA)-overexpressing C2C12 cells subjected to normoxia or hypoxia for 6 hr (n = 5, mean ± SD). *p < 0.01 and **p < 0.0001 (unpaired Student's t test).

(D and E) Representative immunoblots (D) and quantification (E) of PGC1β and TBP (as loading control) protein expression in nuclear extracts from C2C12 myotubes as in (C). Error bars indicate mean ± SD; **p < 0.001 (unpaired Student's t test); ns, not significant.

(F) HREs in the promoter and first intron of the *PGC1β* gene.

(legend continued on next page)

type and metabolic capacity, PGC1β overexpression in muscle increases type IIX myofibers, oxidative capacity, mitochondrial biogenesis, and exercise tolerance (Arany et al., 2007), which presumably should be matched by an increased vascular supply. This is at least the case with other metabolic regulators such as PGC1α and ERRγ, which coregulate aerobic metabolism and angiogenesis in the muscle (Arany et al., 2008; Lin et al., 2002; Narkar et al., 2011). However, our data suggest that PGC1β does not affect the muscle vascular supply in normoxia. How might existing vasculature support PGC1β-mediated metabolic changes? One possibility is that a compensatory vasodilation occurs in the muscle microcirculation to meet metabolic demands. However, we were unable to detect any change in basal blood flow in PGC1β-overexpressing or null skeletal muscles. Notably, exercise, which enhances both muscle oxidative capacity and angiogenesis, only induces coregulators of these phenomena, such as PGC1α, ERRα, and ERRγ, but not PGC1β (Akimoto et al., 2005; Cartoni et al., 2005; Matsakas et al., 2012a). On the other hand, as we have shown, PGC1β is downregulated in hypoxia or ischemia, where lack of oxygen or nutrients would necessitate silencing of oxidative and antiangiogenic gene programs such as those driven by PGC1β (see Figure S7C). Along the same lines, under physiological conditions, PGC1β may serve as a "brake" to prevent uncontrolled and aberrant angiogenesis, which needs to be removed during vascular insufficiency.

Peripheral vascular disease, stroke, and cardiac myopathies are linked to insufficient tissue vascular supply and can benefit from enhanced neoangiogenesis (Baumgartner et al., 2005; Chi et al., 2011; Varu et al., 2010). In contrast, diabetic retinopathy is associated with uncontrolled and aberrant vessel formation, and could be controlled by inhibition of neoangiogenesis (Chung et al., 2010; Costa and Soares, 2013). Despite this prevalent role of angiogenesis in various diseases, molecular regulation of pathological angiogenesis (beyond regulators such as HIF1A) and particularly of the antiangiogenic program remains poorly understood. Here, we have demonstrated that PGC1β drives a net antiangiogenic program by repressing stimulatory angiokines and inducing inhibitory angiokines, which specifically limit ischemic neoangiogenesis. The selectivity of PGC1β-mediated angiostatic effects on ischemia has implications for designing therapies for angiogenesis-linked diseases of muscle and other organs.

EXPERIMENTAL PROCEDURES

All experiments are described in detail in the Supplemental Experimental Procedures.

Animal Husbandry

The mice used in this study were maintained in the vivarium at the Brown Foundation Institute of Molecular Medicine for the Prevention of Human Diseases (UT Medical School) under standard environmental conditions (20–22°C, 12 hr light/12 hr dark cycle) and provided tap water ad libitum. Muscle-specific PGC1β TG male mice (12–14 weeks old) and whole-body PGC1β knockout male mice (16–18 weeks old) were used in the experiments. The muscle-specific PGC1β TG mice were generated in our laboratory on the C57Bl/6J background strain. The whole-body PGC1β knockout mice were obtained from Dr. Evans (Salk Institute). The generation of these PGC1β$^{-/-}$ mice was described previously (Sonoda et al., 2007). In our laboratory, the mice were backcrossed for two generations to the C57Bl/6J background strain. For all rodent experiments, littermate WT mice were always used as controls. The animals were maintained and treated in accordance with the NIH Guide for the Care and Use of Laboratory Animals and with the approval of the Animal Welfare Committee of the University of Texas Health Science Center, Houston.

Cell Culture

C2C12 cells, SVEC4-10 endothelial cells, 293T cells, HUVECs, ARNT^{+} cells, and ARNT^{-} cells were cultured, transfected/infected, and treated as described in the Supplemental Experimental Procedures and as indicated in the figure legends.

Generation of Muscle-Specific PGC1β TG Mice

Muscle-specific PGC1β TG mice were generated using muscle-specific human alpha skeletal actin promoter, mouse PGC1β cDNA, and standard TG techniques as described in the Supplemental Experimental Procedures.

Gene Expression

Total RNA was prepared using the RNeasy Mini Kit (QIAGEN) and analyzed by qPCR using the Applied Biosystems SYBR Green PCR Master Mix with an ABI-7900 cycler (Applied Biosystems). Lists of the qPCR primer sets and sequences used are provided in the Supplemental Experimental Procedures.

PCR-Based Gene Array

PCR arrays were carried out using the mouse Angiogenesis PCR Array (catalog No. PAMM-024; SA Biosciences). The array profiles the expression of 84 genes involved in angiogenesis. PCR array data were analyzed using the online data analysis software from the manufacturer's website.

Protein Extraction and Immunoblotting

The procedures used for nuclear, cytoplasmic, and whole-cell lysate protein extraction, as well as western blotting and the antibodies used, are described in the Supplemental Experimental Procedures.

ChIP Assay

ChIP was performed using ChIP-IT Express (Active Motif) according to the manufacturer's instructions. Details regarding the antibodies used, as well as PCR and qPCR-based detection of binding sites, are provided in the Supplemental Experimental Procedures.

Hindlimb Ischemia, Tissue Collection, and Laser-Doppler Blood Flowmetry

Hindlimb ischemia was induced by unilateral femoral occlusion, and blood flow was measured by laser-Doppler blood flowmetry as described in the Supplemental Experimental Procedures. TA muscles were harvested at the indicated time points after induction of ischemia and processed.

Immunohistochemistry

Immunostaining of skeletal muscle capillaries was performed using CD31 staining in cryosections as described in the Supplemental Experimental Procedures.

Microfil Perfusion and Imaging

Whole-mount vascular imaging of the TA vasculature was performed after microfil angiography as detailed in the Supplemental Experimental Procedures.

(G and H) ChIP-qPCR (G) and ChIP-PCR (H) for the occupancy of HA-tagged HIF1A on *PGC1β* gene (n = 3, mean ± SD). **p < 0.001 (unpaired Student's t test).
(I and J) Luciferase (Luc) activity in 293T cells transfected with the PGC1β first intronic region having either (I) +1,005 HRE or (J) +1,925 HRE or control promoter constructs in pGL3B plasmid (n = 5, mean ± SD). **p < 0.001 (one-way ANOVA).
(K) Model illustrating that PGC1β is a HIF1-regulated transcriptional coregulator that encodes an antiangiogenic gene program and inhibits neoangiogenesis.

Please cite this article in press as: Yadav et al., PGC1β Activates an Antiangiogenic Program to Repress Neoangiogenesis in Muscle Ischemia, Cell Reports (2014), http://dx.doi.org/10.1016/j.celrep.2014.06.040

In Vitro Angiogenesis Assays

In vivo angiogenesis assays, including tube-formation, scratch-migration, and aortic-ring assays, were performed using standard techniques and are detailed in the Supplemental Experimental Procedures.

Microarray Analysis

Genome-wide gene-expression analysis was performed on RNA isolated from TA muscles in WT and TG mice using Illumina Sentrix Beadchip Array Mouse WG-6.v2 arrays. Arrays were scanned with the BeadArray Reader (Illumina). Data were analyzed using GenomeStudio software (Illumina). Clustering and pathway analyses were performed with GenomeStudio and Ingenuity Pathway Analysis (Ingenuity Systems) software, respectively.

Additional experimental procedures are described in the Supplemental Experimental Procedures. Complete lists of the primers and antibodies used are provided in Tables S2–S4.

Statistical Analysis

Data are shown as the mean ± SD. For comparison between two groups, statistical analysis was performed by unpaired Student's t test. For ischemic reperfusion, data were analyzed by two-way ANOVA and Bonferroni's multiple-comparison test. The differences were considered statistically significant at $p < 0.05$.

ACCESSION NUMBERS

Microarray data have been deposited to the NCBI Gene Expression Omnibus under accession number GSE58699.

SUPPLEMENTAL INFORMATION

Supplemental Information includes Supplemental Experimental Procedures, seven figures, and four tables and can be found with this article online at http://dx.doi.org/10.1016/j.celrep.2014.06.040.

AUTHOR CONTRIBUTIONS

V.Y. and V.A.N. designed the experiments, analyzed and interpreted the data, and wrote the manuscript. V.Y., A.M., and S.L. conducted the experiments.

ACKNOWLEDGMENTS

We would like to thank Dr. Ron Evans (Salk Institute, La Jolla) for generously providing the PGC1$\beta^{-/-}$ mice. We would also like to thank Drs. David Loose (UT Microarray Core) and Jeff Chang (UT Bioinformatics Core) for help with microarray analysis. We thank Dr. A.J. Marian (UT) for critically reading the manuscript. This work was supported by UT Health intramural funds, Welch Foundation scholarship funds, and grants from the Muscular Dystrophy Association (MDA#174408), American Heart Association (AHA#11SDG7600213), and American Diabetes Association (ADA#1-13-BS-127).

Received: August 8, 2013
Revised: May 7, 2014
Accepted: June 20, 2014
Published: July 24, 2014

REFERENCES

Akimoto, T., Pohnert, S.C., Li, P., Zhang, M., Gumbs, C., Rosenberg, P.B., Williams, R.S., and Yan, Z. (2005). Exercise stimulates Pgc-1alpha transcription in skeletal muscle through activation of the p38 MAPK pathway. J. Biol. Chem. *280*, 19587–19593.

Arany, Z., Lebrasseur, N., Morris, C., Smith, E., Yang, W., Ma, Y., Chin, S., and Spiegelman, B.M. (2007). The transcriptional coactivator PGC-1beta drives the formation of oxidative type IIX fibers in skeletal muscle. Cell Metab. *5*, 35–46.

Arany, Z., Foo, S.Y., Ma, Y., Ruas, J.L., Bommi-Reddy, A., Girnun, G., Cooper, M., Laznik, D., Chinsomboon, J., Rangwala, S.M., et al. (2008). HIF-independent regulation of VEGF and angiogenesis by the transcriptional coactivator PGC-1alpha. Nature *451*, 1008–1012.

Baumgartner, I., Schainfeld, R., and Graziani, L. (2005). Management of peripheral vascular disease. Annu. Rev. Med. *56*, 249–272.

Cao, Y., Hong, A., Schulten, H., and Post, M.J. (2005). Update on therapeutic neovascularization. Cardiovasc. Res. *65*, 639–648.

Carmeliet, P., and Jain, R.K. (2011). Molecular mechanisms and clinical applications of angiogenesis. Nature *473*, 298–307.

Cartoni, R., Léger, B., Hock, M.B., Praz, M., Crettenand, A., Pich, S., Ziltener, J.L., Luthi, F., Dériaz, O., Zorzano, A., et al. (2005). Mitofusins 1/2 and ERRalpha expression are increased in human skeletal muscle after physical exercise. J. Physiol. *567*, 349–358.

Chi, Y.W., Osinbowale, O., and Milani, R. (2011). Genetic association studies in peripheral arterial disease. J. La. State Med. Soc. *163*, 30–34, 36–37, 39.

Chinsomboon, J., Ruas, J., Gupta, R.K., Thom, R., Shoag, J., Rowe, G.C., Sawada, N., Raghuram, S., and Arany, Z. (2009). The transcriptional coactivator PGC-1alpha mediates exercise-induced angiogenesis in skeletal muscle. Proc. Natl. Acad. Sci. USA *106*, 21401–21406.

Chung, A.S., Lee, J., and Ferrara, N. (2010). Targeting the tumour vasculature: insights from physiological angiogenesis. Nat. Rev. Cancer *10*, 505–514.

Costa, P.Z., and Soares, R. (2013). Neovascularization in diabetes and its complications. Unraveling the angiogenic paradox. Life Sci. *92*, 1037–1045.

Finck, B.N., and Kelly, D.P. (2006). PGC-1 coactivators: inducible regulators of energy metabolism in health and disease. J. Clin. Invest. *116*, 615–622.

Gaudel, C., Schwartz, C., Giordano, C., Abumrad, N.A., and Grimaldi, P.A. (2008). Pharmacological activation of PPARbeta promotes rapid and calcineurin-dependent fiber remodeling and angiogenesis in mouse skeletal muscle. Am. J. Physiol. Endocrinol. Metab. *295*, E297–E304.

Guarani, V., Deflorian, G., Franco, C.A., Krüger, M., Phng, L.K., Bentley, K., Toussaint, L., Dequiedt, F., Mostoslavsky, R., Schmidt, M.H., et al. (2011). Acetylation-dependent regulation of endothelial Notch signalling by the SIRT1 deacetylase. Nature *473*, 234–238.

Han, J.K., Kim, H.L., Jeon, K.H., Choi, Y.E., Lee, H.S., Kwon, Y.W., Jang, J.J., Cho, H.J., Kang, H.J., Oh, B.H., et al. (2013). Peroxisome proliferator-activated receptor-δ activates endothelial progenitor cells to induce angio-myogenesis through matrix metallo-proteinase-9-mediated insulin-like growth factor-1 paracrine networks. Eur. Heart J. *34*, 1755–1765.

Kivelä, R., Silvennoinen, M., Touvra, A.M., Lehti, T.M., Kainulainen, H., and Vihko, V. (2006). Effects of experimental type 1 diabetes and exercise training on angiogenic gene expression and capillarization in skeletal muscle. FASEB J. *20*, 1570–1572.

Lawler, P.R., and Lawler, J. (2012). Molecular basis for the regulation of angiogenesis by thrombospondin-1 and -2. Cold Spring Harb Perspect Med *2*, a006627.

Lekas, M., Lekas, P., Latter, D.A., Kutryk, M.B., and Stewart, D.J. (2006). Growth factor-induced therapeutic neovascularization for ischaemic vascular disease: time for a re-evaluation? Curr. Opin. Cardiol. *21*, 376–384.

Lin, J., Wu, H., Tarr, P.T., Zhang, C.Y., Wu, Z., Boss, O., Michael, L.F., Puigserver, P., Isotani, E., Olson, E.N., et al. (2002). Transcriptional co-activator PGC-1 alpha drives the formation of slow-twitch muscle fibres. Nature *418*, 797–801.

Matsakas, A., Macharia, R., Otto, A., Elashry, M.I., Mouisel, E., Romanello, V., Sartori, R., Amthor, H., Sandri, M., Narkar, V., and Patel, K. (2012a). Exercise training attenuates the hypermuscular phenotype and restores skeletal muscle function in the myostatin null mouse. Exp. Physiol. *97*, 125–140.

Matsakas, A., Yadav, V., Lorca, S., Evans, R.M., and Narkar, V.A. (2012b). Revascularization of ischemic skeletal muscle by estrogen-related receptor-γ. Circ. Res. *110*, 1087–1096.

Milkiewicz, M., Pugh, C.W., and Egginton, S. (2004). Inhibition of endogenous HIF inactivation induces angiogenesis in ischaemic skeletal muscles of mice. J. Physiol. *560*, 21–26.

Muscat, G.E., and Kedes, L. (1987). Multiple 5′-flanking regions of the human alpha-skeletal actin gene synergistically modulate muscle-specific expression. Mol. Cell. Biol. *7*, 4089–4099.

Narkar, V.A., Fan, W., Downes, M., Yu, R.T., Jonker, J.W., Alaynick, W.A., Banayo, E., Karunasiri, M.S., Lorca, S., and Evans, R.M. (2011). Exercise and PGC-1α-independent synchronization of type I muscle metabolism and vasculature by ERRγ. Cell Metab. *13*, 283–293.

O'Hagan, K.A., Cocchiglia, S., Zhdanov, A.V., Tambuwala, M.M., Cummins, E.P., Monfared, M., Agbor, T.A., Garvey, J.F., Papkovsky, D.B., Taylor, C.T., and Allan, B.B. (2009). PGC-1alpha is coupled to HIF-1alpha-dependent gene expression by increasing mitochondrial oxygen consumption in skeletal muscle cells. Proc. Natl. Acad. Sci. USA *106*, 2188–2193.

Olfert, I.M., and Birot, O. (2011). Importance of anti-angiogenic factors in the regulation of skeletal muscle angiogenesis. Microcirculation *18*, 316–330.

Pajusola, K., Künnapuu, J., Vuorikoski, S., Soronen, J., André, H., Pereira, T., Korpisalo, P., Ylä-Herttuala, S., Poellinger, L., and Alitalo, K. (2005). Stabilized HIF-1alpha is superior to VEGF for angiogenesis in skeletal muscle via adeno-associated virus gene transfer. FASEB J. *19*, 1365–1367.

Pereira, F.A., Qiu, Y., Zhou, G., Tsai, M.J., and Tsai, S.Y. (1999). The orphan nuclear receptor COUP-TFII is required for angiogenesis and heart development. Genes Dev. *13*, 1037–1049.

Qin, J., Chen, X., Xie, X., Tsai, M.J., and Tsai, S.Y. (2010). COUP-TFII regulates tumor growth and metastasis by modulating tumor angiogenesis. Proc. Natl. Acad. Sci. USA *107*, 3687–3692.

Rowe, G.C., Jang, C., Patten, I.S., and Arany, Z. (2011). PGC-1β regulates angiogenesis in skeletal muscle. Am. J. Physiol. Endocrinol. Metab. *301*, E155–E163.

Salehi, E., Khazaei, M., and Rashidi, B. (2012). Role of fenofibrate in restoring angiogenesis in diabetic and control hind limb ischemic rats. Gen. Physiol. Biophys. *31*, 255–260.

Sarkar, K., Fox-Talbot, K., Steenbergen, C., Bosch-Marcé, M., and Semenza, G.L. (2009). Adenoviral transfer of HIF-1alpha enhances vascular responses to critical limb ischemia in diabetic mice. Proc. Natl. Acad. Sci. USA *106*, 18769–18774.

Sawada, N., Jiang, A., Takizawa, F., Safdar, A., Manika, A., Tesmenitsky, Y., Kang, K.T., Bischoff, J., Kalwa, H., Sartoretto, J.L., et al. (2014). Endothelial PGC-1α mediates vascular dysfunction in diabetes. Cell Metab. *19*, 246–258.

Semenza, G.L. (2009). Regulation of oxygen homeostasis by hypoxia-inducible factor 1. Physiology (Bethesda) *24*, 97–106.

Semenza, G.L. (2012). Hypoxia-inducible factors in physiology and medicine. Cell *148*, 399–408.

Simons, M., and Ware, J.A. (2003). Therapeutic angiogenesis in cardiovascular disease. Nat. Rev. Drug Discov. *2*, 863–871.

Sonoda, J., Mehl, I.R., Chong, L.W., Nofsinger, R.R., and Evans, R.M. (2007). PGC-1beta controls mitochondrial metabolism to modulate circadian activity, adaptive thermogenesis, and hepatic steatosis. Proc. Natl. Acad. Sci. USA *104*, 5223–5228.

van Weel, V., van Tongeren, R.B., van Hinsbergh, V.W., van Bockel, J.H., and Quax, P.H. (2008). Vascular growth in ischemic limbs: a review of mechanisms and possible therapeutic stimulation. Ann. Vasc. Surg. *22*, 582–597.

Varu, V.N., Hogg, M.E., and Kibbe, M.R. (2010). Critical limb ischemia. J. Vasc. Surg. *51*, 230–241.

Wood, S.M., Gleadle, J.M., Pugh, C.W., Hankinson, O., and Ratcliffe, P.J. (1996). The role of the aryl hydrocarbon receptor nuclear translocator (ARNT) in hypoxic induction of gene expression. Studies in ARNT-deficient cells. J. Biol. Chem. *271*, 15117–15123.

Zhang, H., Gao, P., Fukuda, R., Kumar, G., Krishnamachary, B., Zeller, K.I., Dang, C.V., and Semenza, G.L. (2007). HIF-1 inhibits mitochondrial biogenesis and cellular respiration in VHL-deficient renal cell carcinoma by repression of C-MYC activity. Cancer Cell *11*, 407–420.

Cell Reports, Volume *8*

Supplemental Information

PGC1β Activates an Antiangiogenic Program to Repress Neoangiogenesis in Muscle Ischemia

Vikas Yadav, Antonios Matsakas, Sabina Lorca, and Vihang A. Narkar

SUPPLEMENTAL FIGURE LEGENDS

FIGURE S1. *Vegfa* and Cytochrome c (*Cycs*) expression. (A-B) Relative gene expression of PGC1β target gene *Cycs* (A) and *Vegfa* isoforms *Vegf121*, *Vegf165* and *Vegf189* (B) (N=6, mean ± SD). ** p<0.00001 (unpaired student's t-test). **(C)** Representative immunoblots for VEGA and β-tubulin (loading control) in cytoplasmic fraction obtained from control and PGC1β over-expressing C2C12 myotubes (N=3). Related to Figure 1.

FIGURE S2. Muscle-specific Pgc1β transgenic mice. (A) The human alpha skeletal actin promoter (HSA)-*PGC1β-BGHpolyA* transgene construct was cloned in pBluescript II KS (+) plasmid, as shown. **(B)** pBluescript II KS (+) plasmid map containing transgene construct HSA- *PGC1β*-BGHpolyA. Green arrows mark the restriction enzymes used to excise the transgene from the plasmid for microinjection. **(C)** Digestion of recombinant plasmid pBSK-HSA-*PGC1β*-BHGpolyA with *Pvu1* and *Kpn1* restriction enzymes demonstrating the excision of the 6 kb transgene for microinjection. **(D)** Genotyping of mice obtained after microinjection (total 11 pups) for the presence of transgene. Related to Figure 2.

FIGURE S3. Characterization of muscle-specific PGC1β transgenic mice. (A) Relative mRNA expression of PGC1β in tibialis anterior (TA), soleus (SOL), quadriceps (QUADS) and gastrocnemius (GASTROC) muscles from muscle-specific PGC1β transgenic mice (TG) compared to wild type (WT) littermates (N=5, mean ± SD). * p<0.0001 (unpaired student's t-test). **(B)** Representative western blots for PGC1β and

β-tubulin (as loading controls) in muscle extracts from TA and GASTROC from TG and WT mice. **(C-E)** Relative mRNA expression of genes involved in fiber type, oxidative phosphorylation (OXPHOS) and fatty acid oxidation (FAO) in TA form WT and TG mice. (N=5, mean ± SD). * $p<0.001$ (unpaired student's t-test). **(F)** Representative western blots for myoglobin, Cycs, MHCIIx and β-tubulin (as loading controls) in GASTROC from TG and WT mice. **(G)** Relative amount mitochondrial DNA in QUADS and GASTROC muscles from TG and WT mice (N=5, mean ± SD). * $p<0.01$ (unpaired student's t-test). **(H)** Representative images of SDH staining of TA cryosections from TG and WT mice (N=3). **(I)** Gross phenotypic comparison between the TG and WT mice. **(J)** Representative images of H&E stained TA cryosections from TG and WT mice (N=3). **(K)** Serum creatine kinase levels in TG and WT mice (N=6, ns is not significant). Related to Figure 2.

FIGURE S4. (A) Tube formation in human umbilical vein endothelial cells (HUVEC) treated with TA muscle extracts from wild type (WT) and transgenic (TG) mice. *Right panel.* Quantification of tube formation presented as number of tubes per well (N=3, mean ± SD). *$p<0.001$ (unpaired student's t-test). **(B)** CD31-stained capillaries in TA muscles from WT and TG mice (Representative from N=3 experiments). Related to Figure 2.

FIGURE S5. Global gene expression. (A) Pie chart showing up or down-regulated genes in TA from transgenic mice. **(B)** Regulation of VEGF signaling pathway genes by PGC1β in TA. All changes are two fold or more. $p<0.05$. Related to Figure 2.

FIGURE S6. Relative mRNA expression of COUP-TF1 and COUP-TFII in C2C12 myotubes (N=5, mean ± SD). *p<0.05 (unpaired student's t-test). Related to Figure 5.

FIGURE S7. (A) Relative gene expression of *Pgc1β* and hypoxia-regulated genes (VEGFD, NOS2, VEGFA and PDGFβ) in human umbilical vein endothelial cells (HUVEC) subjected to hypoxia (H) or normoxia (N) for 6 h. **(B)** Relative gene expression of indicated genes in murine endothelial SVEC4-10 cells (N=6, mean ± SD). * p<0.00001, ** p<001 (unpaired student's t-test). Related to Figure 6. **(C)** Relative expression of metabolic genes in contralateral and ischemic gastrocnemius muscles from the WT and PGC1β-/- mice (N=4). * p<0.05, unpaired Student's t-test. Related to Discussion.

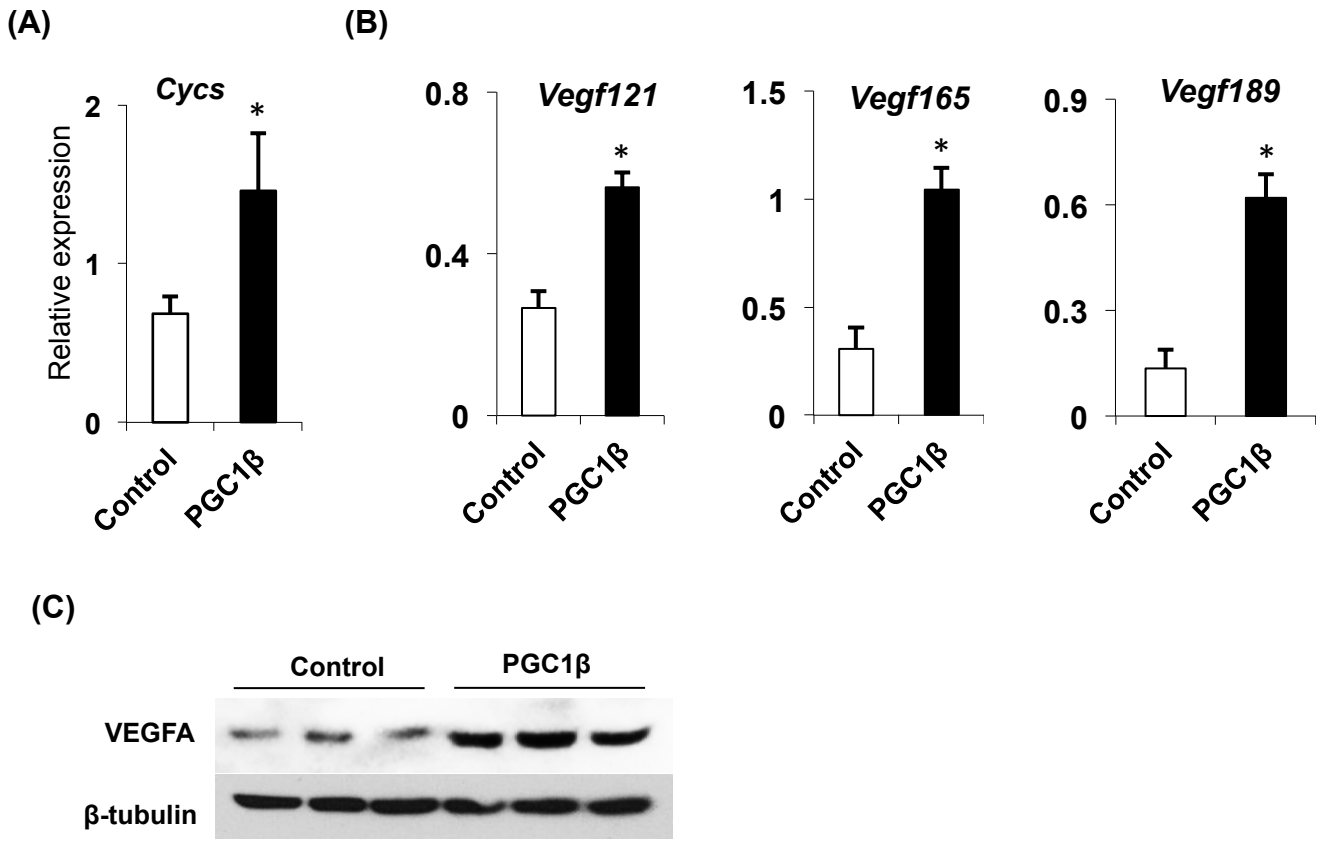
(A)
(B)
Cycs
Vegf121
Vegf165
Vegf189
Relative expression
2
1
0
0.8
0.4
1.5
0.5
0.9
0.6
0.3
*
Control
PGC1β
(C)
Control
PGC1β
VEGFA
β-tubulin

FIGURE S1

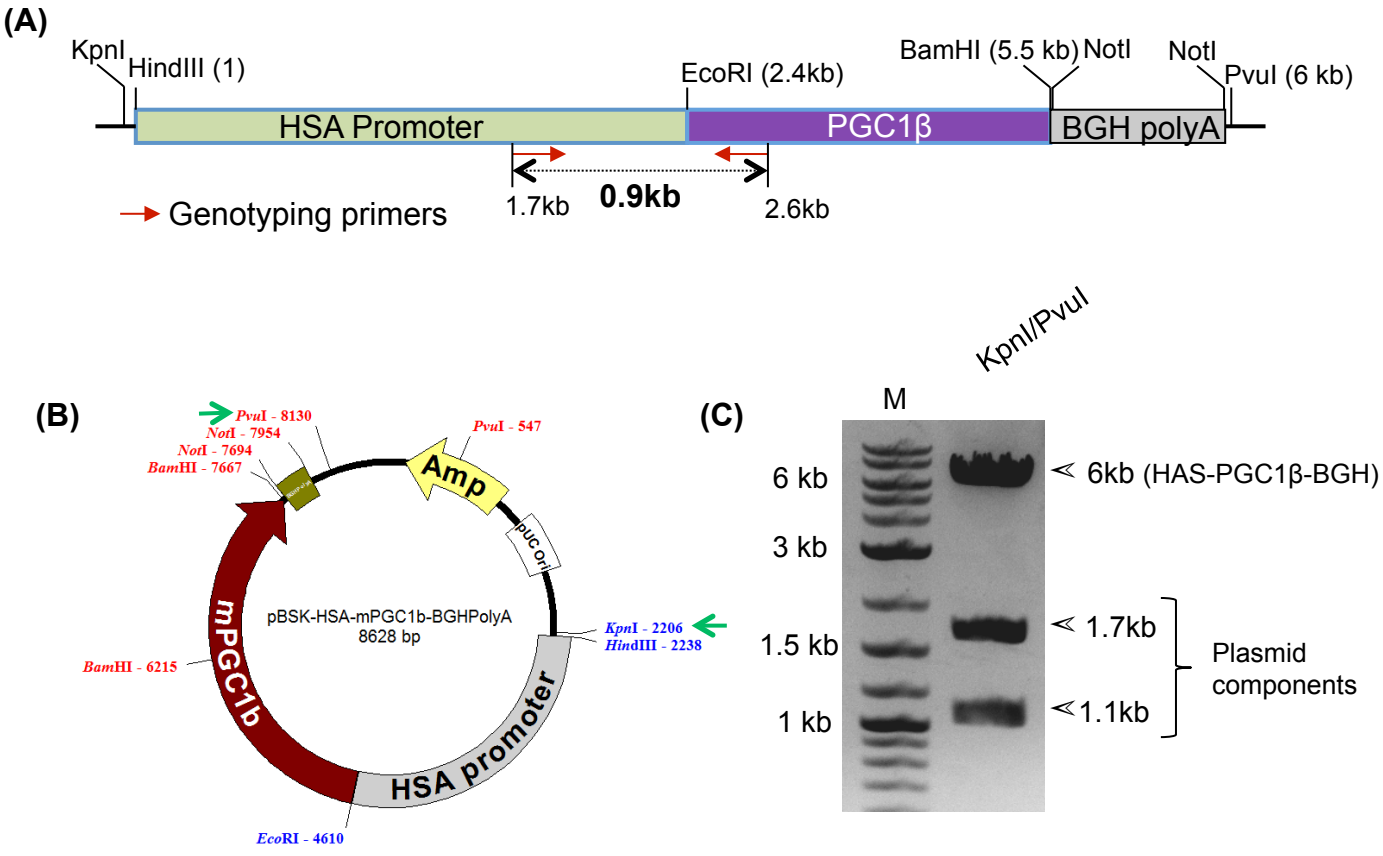
(A)
KpnI
HindIII (1)
EcoRI (2.4kb)
BamHI (5.5 kb)
NotI
NotI
PvuI (6 kb)
HSA Promoter
PGC1β
BGH polyA
Genotyping primers
1.7kb
0.9kb
2.6kb
(B)
PvuI - 8130
NotI - 7954
NotI - 7694
BamHI - 7667
PvuI - 547
Amp
puc ori
pBSK-HSA-mPGC1b-BGHPolyA
8628 bp
KpnI - 2206
HindIII - 2238
BamHI - 6215
mPGC1b
HSA promoter
EcoRI - 4610
(C)
KpnI/PvuI
M
6 kb
3 kb
1.5 kb
1 kb
6kb (HAS-PGC1β-BGH)
1.7kb
1.1kb
Plasmid components
(D)
Marker
1
2
3
4
5
6
7
8
9
10
11
1kb
0.9kb

FIGURE S2

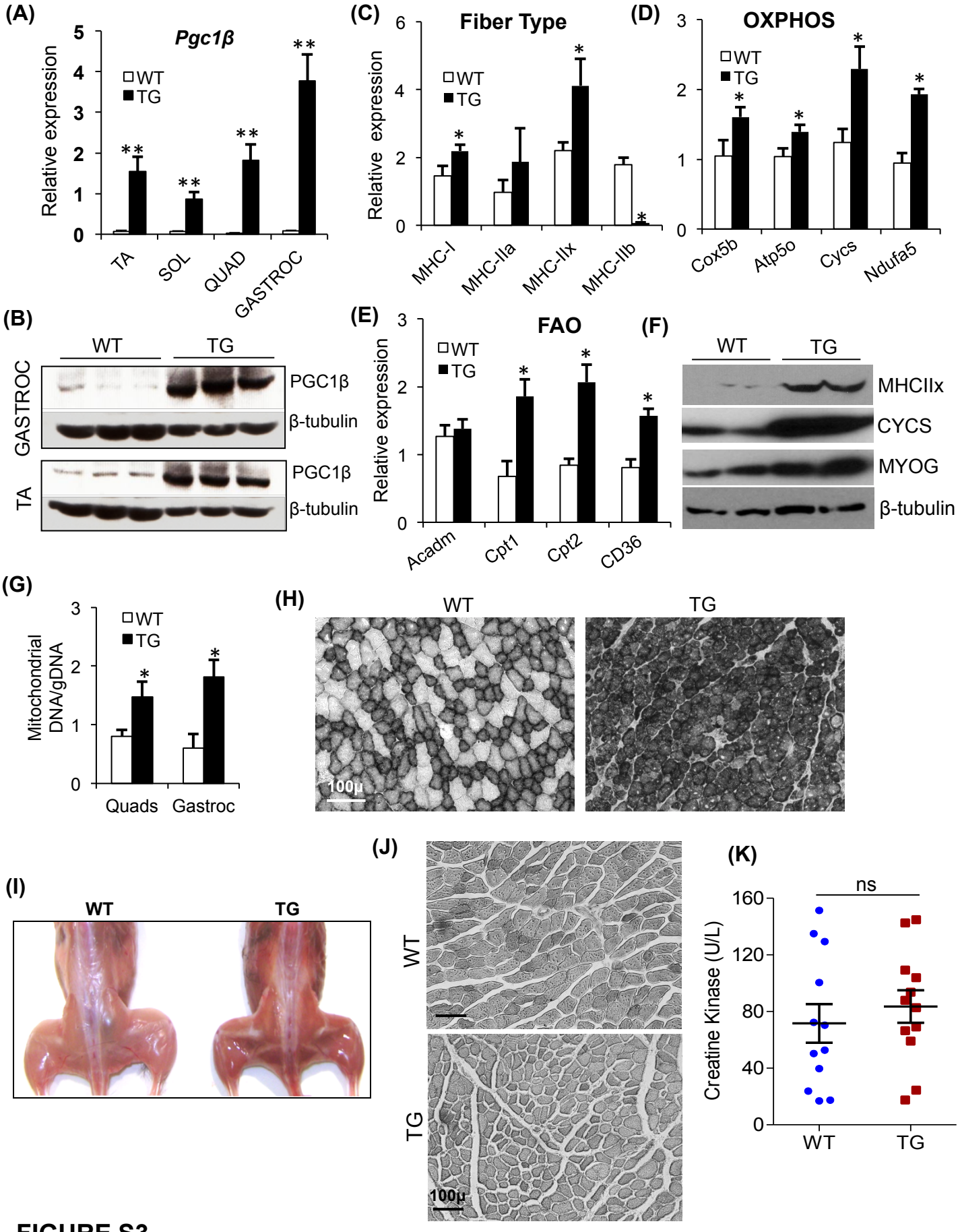
(A)
Pgc1β
Relative expression
WT
TG
TA
SOL
QUAD
GASTROC
(B)
WT
TG
GASTROC
PGC1β
β-tubulin
TA
PGC1β
β-tubulin
(C)
Fiber Type
Relative expression
MHC-I
MHC-IIa
MHC-IIx
MHC-IIb
(D)
OXPHOS
Cox5b
Atp5o
Cycs
Ndufa5
(E)
FAO
Acadm
Cpt1
Cpt2
CD36
(F)
MHCIIx
CYCS
MYOG
β-tubulin
(G)
Mitochondrial DNA/gDNA
Quads
Gastroc
(H)
100μ
(I)
(J)
100μ
(K)
Creatine Kinase (U/L)
ns

FIGURE S3

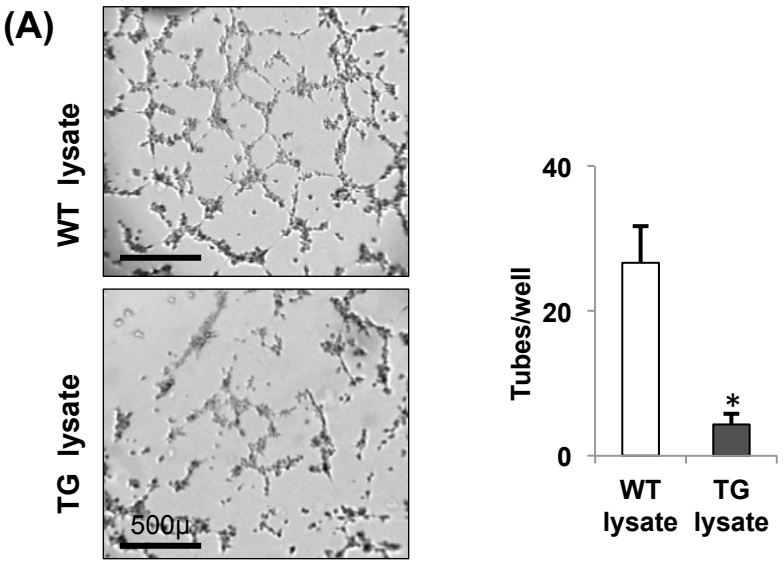
(A)
WT lysate
TG lysate
500μ
Tubes/well
40
20
0
*
WT lysate
TG lysate

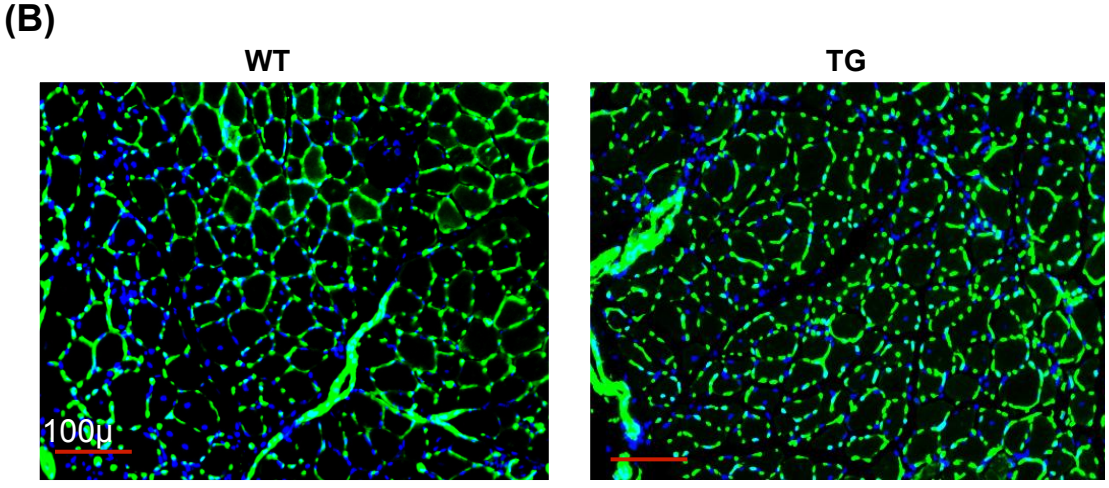
(B)
WT
TG
100μ

FIGURE S4

(A)

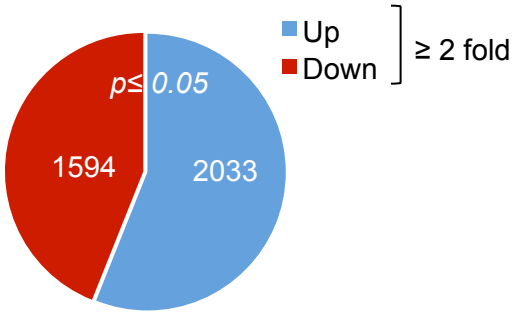

(B)

Gene	fold change	*p* value	Gene ID	Gene Name
MAPK12	-2.66	3E-11	NM_013871.2	Mus musculus mitogen-activated protein kinase 12 (Mapk12), mRNA.
PPP3CA	-2.04	3.5E-35	NM_008913.3	Mus musculus protein phosphatase 3, catalytic subunit, alpha isoform (Ppp3ca), mRNA.
NFATC1	-2.79	0.00137	NM_016791.3	Mus musculus nuclear factor of activated T-cells, (Nfatc1), transcript variant 1, mRNA.
MAPK12	-2.60	7.4E-38	NM_013871.2	Mus musculus mitogen-activated protein kinase 12 (Mapk12), mRNA.
MAPK12	-2.84	7.4E-38	NM_013871.2	Mus musculus mitogen-activated protein kinase 12 (Mapk12), mRNA.
NFATC3	-2.23	7.4E-38	NM_010901.2	Mus musculus nuclear factor of activated T-cells, cytoplasmic, calcineurin-dependent 3 (Nfatc3), mRNA.
NFATC1	-2.35	0.00661	NM_016791	
PLA2G12A	-2.25	1E-07	NM_023196	
NFATC1	-2.16	3.1E-19	NM_198429.1	Mus musculus transcript nuclear factor of activated T-cells, (Nfatc1), variant 2, mRNA.
PLA2G6	-2.69	5.3E-16	NM_016915.3	Mus musculus phospholipase A2, group VI (Pla2g6), mRNA.
DNAJC12	-2.28	1.4E-23	NM_013888.2	Mus musculus DnaJ (Hsp40) homolog, subfamily C, member 12 (Dnajc12), mRNA.
PLA2G12A	-2.23	7.4E-38	NM_023196.2	Mus musculus phospholipase A2, group XIIA (Pla2g12a), transcript variant 1, mRNA.
PPP3CB	-2.67	7.4E-38	NM_008914	
NFATC1	-2.17	1.5E-30	NM_198429.1	Mus musculus nuclear factor of activated T-cells, (Nfatc1), transcript variant 2, mRNA.

FIGURE S5

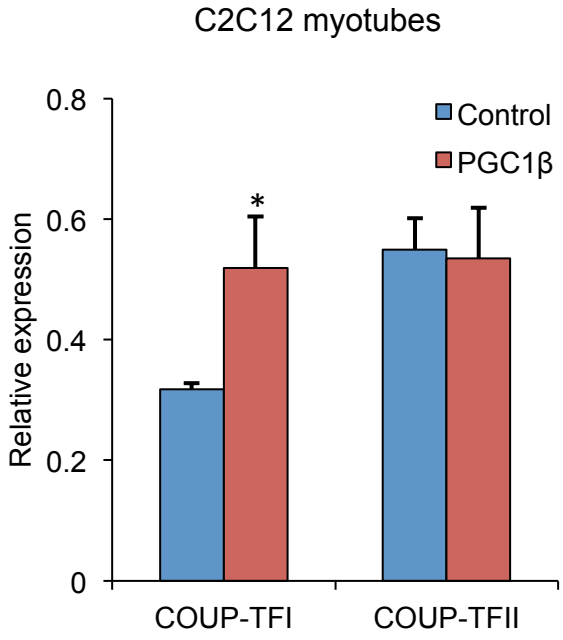
C2C12 myotubes
Relative expression
0.8
0.6
0.4
0.2
0
Control
PGC1β
*
COUP-TFI
COUP-TFII

FIGURE S6

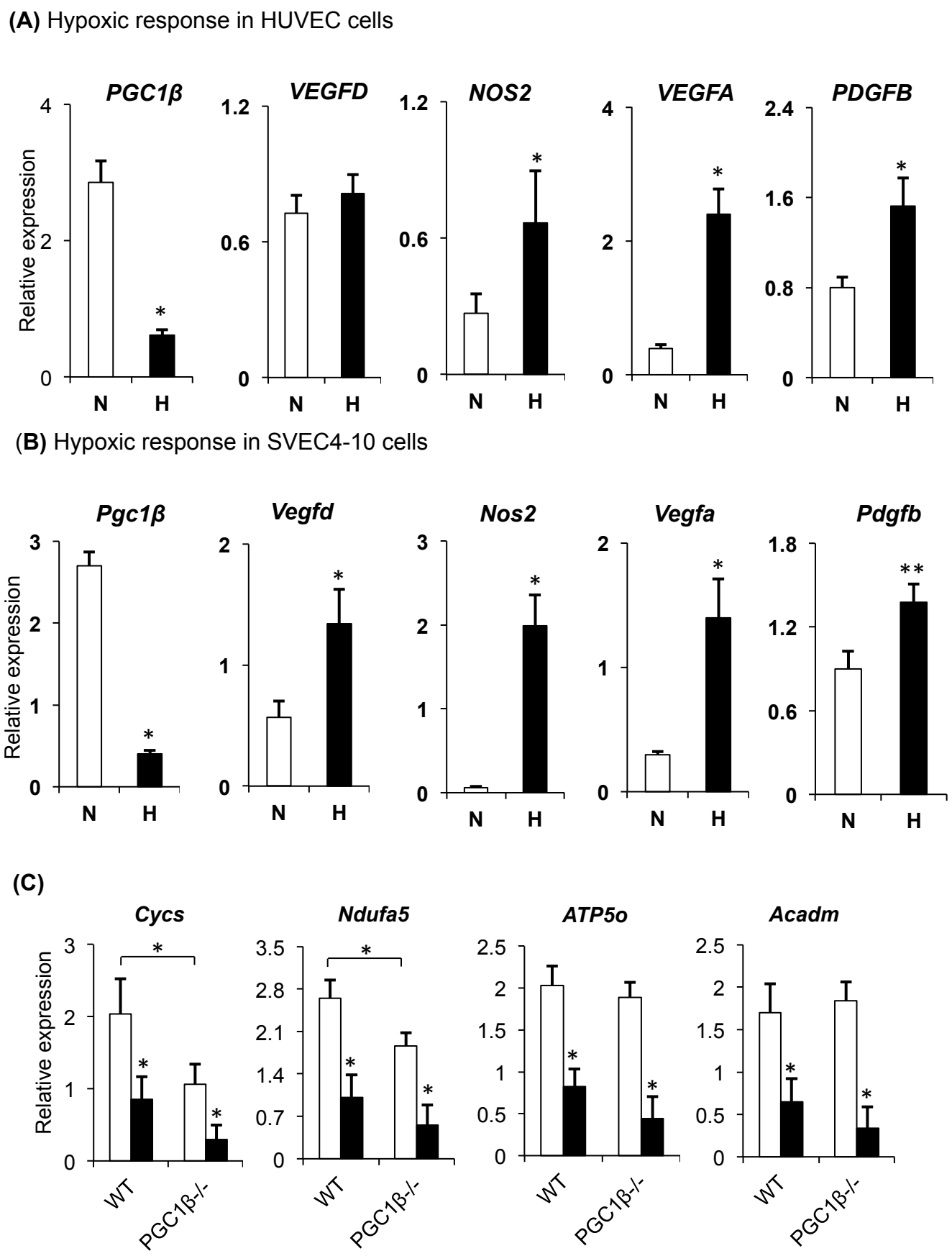
(A) Hypoxic response in HUVEC cells
PGC1β
VEGFD
NOS2
VEGFA
PDGFB
Relative expression
N
H
(B) Hypoxic response in SVEC4-10 cells
Pgc1β
Vegfd
Nos2
Vegfa
Pdgfb
(C)
Cycs
Ndufa5
ATP5o
Acadm
WT
PGC1β-/-
Control limb
Ischemic limb

FIGURE S7

SUPPLEMENTAL TABLES

Table S1. Angiogenic gene regulation by PGC1β. Fold up or down regulation of angiogenic genes in C2C12 myotubes overexpressing PGC1β using PCR-array for angiogenesis.

Gene Symbol	Fold change vs. control	Gene Symbol	Fold change vs. control	Gene Symbol	Fold change vs. control	Gene Symbol	Fold change vs. control
Angpt1	-10.623	Ephb4	-1.946	Kdr	1.117	Sphk1	-2.144
Angpt2	-9.367	Ereg	2.028	Lama5	-1.201	Stab1	-1.008
Anpep	-4.818	F2	6.444	Lect1	-2.095	Tbx1	-1.052
Bai1	-1.065	Fgf1	-4.233	Lep	1.051	Tbx4	6.927
Ccl11	-3.743	Fgf2	-1.834	Mapk14	1.022	Tek	-1.377
Ccl2	-13.924	Fgf6	-1.276	Mdk	1.080	Tgfa	-1.065
Cdh5	-2.068	Fgfr3	3.962	Mmp19	1.404	Tgfb1	-2.236
Col18a1	1.300	Figf	-20.542	Mmp2	-2.762	Tgfb2	1.130
Col4a3	1.381	Flt1	1.025	Mmp9	1.094	Tgfb3	1.600
Csf3	1.033	Fzd5	1.525	Npr1	-4.946	Tgfbr1	-1.216
Ctgf	-5.298	Gna13	-1.079	Nrp1	-2.294	Thbs1	-6.594
Cxcl1	-5.345	Hand2	1.630	Nrp2	-1.043	Thbs2	3.062
Cxcl2	-1.065	Hgf	-2.993	Pdgfa	1.005	Timp1	-1.672
Cxcl5	-8.980	Hif1a	1.109	Pecam1	-2.686	Timp2	-2.557
Tymp	-1.297	Ifng	-4.175	Pgf	-1.634	Tmprss6	-3.523
S1pr1	-1.454	Igf1	-5.446	Plau	-2.419	Tnf	1.380
Efna1	-1.126	Il1b	-12.318	Plg	-1.435	Tnfaip2	1.248
Efnb2	-1.504	Il6	-1.105	Plxdc1	-6.302	Tnfsf12	-6.548
Egf	1.127	Itgav	-1.478	Ptgs1	-1.709	Vegfa	2.402
Eng	-2.103	Itgb3	-1.861	Serpinf1	1.069	Vegfb	-2.173
Epas1	1.076	Jag1	1.457	Smad5	-1.088	Vegfc	-9.057

Table S2. Mouse QPCR primer list.

Prime Name	Forward primer	Reverse primer
Ang1	CATTCTTCGCTGCCATTCTG	GCACATTGCCCATGTTGAATC
Ang2	TTAGCACAAAGGATTCGGACAAT	TTTTGTGGGTAGTACTGTCCATTCA
Angiostatin 1	TGCAGTGGAGAAAAGTATGAGGG	AGGGATGTATCCATGAGCATGT
Atp5o	TCTCGACAGGTTCGGAGCTT	AGAGTACAGGGCGGTTGCATA
CD36	CTGGGACCATTGGTGATGAAA	CACCACTCCAATCCCAAGTAAG
Coup-TF1	GCACTACGGCCAATTCACCT	TTGGAGGCATTCTTCCTCGC
Coup-TFII	GGTCTGTCTGATGTAGCCCAT	GGCTCCTAACGTACTCTTCCAA
Cox5b	TTCAAGGTTACTTCGCGGAGT	CGGGACTAGATTAGGGTCTTCC
CPT1	CACCAACGGGCTCATCTTCTA	CAAAATGACCTAGCCTTCTATCGAA
CPT2	CAAAAGACTCATCCGCTTTGTTC	CATCACGACTGGGTTTGGGTA
Cyclophilin	TGGAGAGCACCAAGACAGACA	TGCCGGAGTCGACAATGAT
Cycs	CCAAATCTCCACGGTCTGTTC	ATCAGGGTATCCTCTCCCCAG
Endostatin	GTGCCCATCGTCAACCTGAA	GACATCTCTGCCGTCAAAAGAA
Fgf1	GAAGCATGCGGAGAAGAACTG	CGAGGACCGCGCTTACAG
Fgf2	CACCAGGCCACTTCAAGGA	GATGGATGCGCAGGAAGAA
MCAD	AGGGTTTAGTTTTGAGTTGACGG	CCCCGCTTTTGTCATATTCCG
MHC-I	CTCCAGGCTGCTTTAGAGGAA	CCTGCTCCTAATCTCAGCATCC
MHC-IIa	AAGCGAAGAGTAAGGCTGTC	CTTGCAAAGGAACTTGGGCTC
MHC-IIb	GAAGAGCCGAGAGGTTCACAC	CAGGACAGTGACAAAGAACGTC
MHC-IIx	GAAGAGTGATTGATCCAAGTG	TATCTCCCAAAGTTATGAGTA
Ndufa5	AGCTGGATATGGTCAAGGCG	GCCACTTCCACTGGTTAGCA
Nos2	CAGCTGGGCTGTACAAACCTT	CATTGGAAGTGAAGCGTTTCG
Pdgf-β	TGTTCCAGATCTCGCGGAAC	GCGGCCACACCAGGAAG
Pedf	GCCCTGGTGCTACTCCTCT	CGGATCTCAGGCGGTACAG
Pgc1β	TCCTGTAAAAGCCCGGAGTAT	GCTCTGGTAGGGGCAGTGA
Tsp1	ACTACGCTGGCTTTGTTTTC	GGACTGGGTGACTTGTTTCC
Tsp2	CTGGGCATAGGGCCAAGAG	GTCTTCCGGTTAATGTTGCTGAT
Vashohibin	ACATGCGGCTCAAGATTGG	CTCTGGGGAGGAAACATCCTT
Vegf121	TGCAGGCTGCTGTAACGATG	CCTCGGCTTGTCATTTTTCT
Vegf165	TGCAGGCTGCTGTAACGATG	GAACAAGGCTCACAGTGATTTTCT

Vegf189	TGCAGGCTGCTGTTAACGATG	CTCCAGGATTTAAACCGGGATT
Vegfc	AAGACCGTGTGCGAATCGA	CACAGCGGCATACTTCTTCACT
Vegfd	AAATCGCGCACTCTGAGGA	TGGCAAGACTTTTGAGCTTCAA

Table S3. Human QPCR primer list.

Prime Name	**Forward primer**	**Reverse primer**
PGC1β	CGCTTTGAAGTGTTTGGTGAGATTG	GCTGGAAGGAGGGCTCGTTG
VEGFD	CGATGTGGTGGCTGTTGCAATGAA	GCTGTTGGCAAGCACTTACAACCT
VEGFA	GAAGTGGTGAAGTTCATGGATGTCTAT	TCAGGGTACTCCTGGAAGATGTC
PDGFβ	GCCGAGTTGGACCTGAACAT	TCTTGCACTCGGCGATCAT
NOS2	TCAAATCTCGGCAGAATCTACAAA	CAGGAGAGTTCCACCAGGATG

Table S4. Antibodies used.

Antibody	Source/Catalogue number	Purpose/ Working dilution
Anti-PGC1β	R&D Systems/AF5656	WB/1:1000 in 5% milk
Anti-HA	Cell Signaling/29F4	WB/1:1000 in 5% BSA ChIP/1:100
Anti vegfa	Abcam/ab46154	WB/1:2000 in 5% milk
Anti-beta tubulin	Abcam/ab6046	WB/1:5000 in 5% milk
Anti TBP (TATA binding protein)	Abcam/ab818	WB/1:2500 in 5% milk
Anti-iNOS	Cell Signaling/2977	WB/1:1000 in 5% BSA
Anti-Cycs	BD Pharmingen/556433	WB/1:2000 in 5% milk
Anti-MHCIIX	Developmental Studies Hybridoma Bank/6H1	WB/1:200 in 5% milk
Anti-myoglobin	Santacruz Biotechnology/SC-25607	WB/1:2500 in 5% milk
Anti-COUP-TF1	Cell Signaling/6364	WB/1:1000 in 5% BSA
Anti-TSP1	Thermo Scientific/MS-419	WB/1:400 in 5% BSA
Anti-TSP2	BD Bioscience/611150	WB/1:500 in 5% BSA
Anti-FGF2	Millipore/05-118	WB/1:1000 in 5% milk
Anti-PEDF	R&D Systems/AF1149	WB/1:250 in 5% milk
Anti-Endostatin	R&D Systems/AF570	WB/1:400 in 5% milk
Anti-His tag	Cell Signaling/2366	IP/ 1:100
Goat anti rabbit IgG-HRP secondary	Santacruz Biotechnology/SC-2004	WB/1:3000 in 5% BSA
Donkey anti goat IgG-HRP secondary	Santacruz Biotechnology/SC-2020	WB/1:3000 in 5% BSA
Goat anti mouse IgG-HRP secondary	Santacruz Biotechnology/SC-2005	WB/1:5000 in 5% BSA

SUPPLEMENTAL EXPERIMENTAL PRODEDURES

Cell culture

C2C12 cells were cultured in DMEM with 20% FBS and normocin (Invitogen). SVEC4-10 endothelial cells (ATCC# CRL-2181) and 293T cells (ATCC# CRL-11268) were cultured in DMEM with 10% FBS and normocin. HUVEC cells were cultured in endothelial basal media bullet kit (Lonza). $ARNT^+$ (ATCC# CRL-2712) and $ARNT^-$ (ATCC# CRL-2717) cells were cultured in MEMα with 2mM L-glutamine (Invitrogen) in the presence or absence of G418 (Sigma), respectively. For the differentiation of C2C12 cells into myotubes, DMEM containing 2% horse serum was used.

Hypoxia and hypoxia mimetic Dimethyloxaloylglycine (DMOG) treatment

The cells were subjected to hypoxia in the Modular Incubator Chamber. A pre-analyzed gas mixture of 5% CO_2 and 95% N_2 was flushed through the Modular Incubator Chamber containing the cultured cells at the flow rate of 20 liters/min for 5 min. The chamber containing the cells in the hypoxic environment was maintained in the regular cell culture incubator at 37°C for 6 h. For hypoxia mimetic studies, the cells were treated with 1mM DMOG for 24 h.

PGC1β over-expression in C2C12 cells

C2C12 cells were transfected with pCDNA-PGC1β or empty vector (pcDNA) using Lipofectamine 2000 (Invitrogen) in 10 cm^2 culture plates. Forty-eight hours post-transfection, G418 (Sigma) was added at concentrations of 0.6 mg/ml to the cells. Medium was replaced every 48 h with fresh DMEM (+20% FBS) containing 0.6mg/ml

G418. After one week, individual clones were picked and propagated for 5-7 days in 24-well plate in presence of 0.6 mg/ml G418 followed by sub-culturing them in 6-well tissue culture plate. All clones were cultured for at least two week in the presence of G418 before screening them by PCR. To confirm the presence of the construct in the genome, PCR was performed using genomic DNA as template and primer pairs PGC1β-F: atgacaccgtatttgaggacagcagcagca and PGC1β-R: gaatagaatgacacctactcagacaatgcga followed by QPCR to evaluate the functional expression of PGC1β and its known target gene *Cycs* compared to empty vector control cells.

PGC1β overexpression in SVEC4-10 cells

We used lentivirus particles to generate PGC1β overexpressing SVEC4-10. Third generation lentivirus packaging plasmid system was used. PGC1β was cloned in the lentivirus plasmid pLenti-CMV-GFP-Puro (addgene # 17448) between XbaI and SalI sites and used for the transfection of HEK293T cells together with plasmids pRSV-Rev (addgene #12253), pMDLg/pRRE (addgene # 12251) and pMD2.G (addgene # 12259) using Lipofectamine 2000 (Invitrogen). Virus-containing supernatants were collected at 48 h after transfection and concentrated using Lenti-Pac™ lentivirus concentration solution (GeneCopoeia) and used to transduce the cells for 12 h in the presence of 8 µg/ml polybrene (Millipore). Forty-eight hours post-transduction, cells were incubated with standard growth medium containing 2µg/ml puromycin (Sigma) for 3-5 days to select stable cells prior to analysis.

Generation of muscle-specific PGC1β transgenic mice

The PGC1β coding sequence was cloned in pBSK-HSA plasmid at EcoRI and BamHI sites followed by cloning of bovine growth hormone (BHG) poly-adenylation signal sequence at Not I site to 3' of the PGC1β. The transgene construct was sequenced to confirm its presence of all components in right order and was excised from pBSK-HSA-PGC1β plasmid by digesting with KpnI and PvuI restriction enzymes. DNA was microinjected into fertilized oocytes of F1 mice (C57BL/6J). Screening of founder mice and their offspring for stable transmission through the germline was done by PCR. DNA was extracted from tail biopsy using genomic DNA extraction kit from Clontech. A 900bp fragment corresponding to the transgene was PCR amplified using the primer pair PGC1βgenoF: atgcagctaagagaccatgagat and PGC1βgenoR: atagtcagtgtatctgggccaac, and further confirmed by sequencing.

Gene expression

Total RNA was prepared using the RNeasy Mini Kit (Qiagen), and was further (5 µg) reverse-transcribed to cDNA with SuperScript II^{TM} Reverse Transcriptase (Invitrogen), and analyzed by QPCR using the Applied Biosystems SYBR Green PCR Master Mix using an ABI-7900 cycler (Applied Biosystems). Primes used are shown **Table S2** and **S3** and were designed using the software Primer Express 3.0 (Applied Biosystems). All data were normalized to cyclophilin. For the gene expression studies in aortic ring explants, relative amount of mRNA was calculated using comparative Ct (ΔCt) method.

PCR-based gene array

PCR arrays were carried out using the mouse Angiogenesis PCR Array (cat # PAMM-024; SA Biosciences, Frederick, MD, USA). The array profiles the expression of 84 genes involved in angiogenesis. Briefly, total RNA was extracted from C2C12 myotubes overexpressing PGC1β or control cells using Trizol reagent (Life Technologies). Total RNA from n=2 biological samples/group was pooled such that there were 3 biological replicates/group, and was further processed to obtain cDNA using RT^2 first strand cDNA synthesis kit (SA Biosciences). The cDNA was subjected to the PCR array, as per manufacturer's instructions (SA Biosciences) for ABI Prism 7900 HT sequence detection system. PCR array data were analyzed using the online data analysis software from the manufacturer's website to identify gene expression changes (http://www.sabiosciences.com/pcrarraydataanalysis.php). Four housekeeping genes (*HSP90ab1*, *ACTB*, β-*2 microglobulin*, and β-*glucouronidase*) were used to normalize the data. Fold up or down regulation of individual genes was calculated for PGC1β overexpressing group compared to control cells (empty vector).

Protein extraction and immunoblotting

Nuclear extracts (NE) and cytoplasmic extracts (CE) were prepared using NE-PER Nuclear and Cytoplasmic extraction reagents (Thermo Scientific) in the presence of protease inhibitor cocktail (Roche). For whole cell lysate, cells were lysed with Pierce® IP lysis buffer (Thermo Scientific) containing protease inhibitor cocktail (Roche) while for whole tissue lysates, tissues were homogenized at 4°C at maximum speed using a homogenizer (Polytron) in presence of Pierce® IP lysis buffer containing protease inhibitor cocktail (Roche). Cell debris was pellet down by centrifugation at 13000 rpm for

15 min at 4°C. All protein samples were quantified by Pierce BCA protein assay kit (Thermo Scientific). Western blot analysis was performed using standard protocols. The primary and secondary antibodies used for western blots are shown in **Table S4**.

Chromatin immunoprecipitation (ChIP) assay

ChIP assays were performed using C2C12 cells in 15 cm dishes. C2C12 cells were transfected with HA-tagged HIF1A (HA-HIF1A) using Lipofectamine 2000. Forty-eight hours post-transfection, cells were subjected to 6 h of hypoxia. ChIP was performed using ChIP-IT express (Active Motif) according to the manufacturer's instructions. Twenty microgram of enzymatically sheared chromatin was pre-cleared with protein A/G beads and immunoprecipitated using anti-HA monoclonal antibodies (Cell signaling) and protein G magnetic beads for 4 h at 4°C. The sheared DNA-protein complexes were incubated overnight at 65°C for reverse cross-linking and then treated with protease K followed by column purification (Active Motif). Purified DNA fragments were subjected to PCR and QPCR. The PCR for the hypoxia responsive elements (HRE) in PGC1β promoter region and in the first intron was performed using the primers shown in **Table S3**. For the occupancy of PGC1β on THBS1 and THBS2 promoter regions via COUP-TF1, ChIP was performed with C2C12 cells transfected with either histidine tagged PGC1β (PGC1β-HIS) or empty vector. ChIP was performed as mentioned above. The PCR and QPCR were performed using the primers shown in **Table S3**.

Transient reporter assay

Promoter fragments were sub-cloned into pGL3-Basic luciferase reporter plasmid (Promega). In 96-well plate, 293T cells were transfected with Lipofectamine 2000 (Invitrogen) with 150 ng DNA/well, as indicated in the figures. Reporter gene assays were performed at 48 h post transfection with the Dual-luciferase reporter assay system (Promega). pRL-TK (Promega) *renilla* luciferase (10 ng) was co-transfected in each sample as an internal control for transfection efficiency and for data normalization.

Tube formation assay

HUVEC cells were suspended in EBM medium (without supplements) containing 0.5μg/μl crude tissue lysates of TA from wild type or PGC1β transgenic mice. $1x10^4$ HUVEC cells were seeded in 94-well coated with BD-Matrigel™ (reduced growth factor). Endothelial network formation was assessed at 3 h after cell seeding and was quantified in randomly captured microscopic fields (5X magnification) by counting the number of intersection points and calculating the number of tubes per well and plotted.

Hindlimb ischemia and tissue collection

Hindlimb ischemia was induced by unilateral femoral occlusion, as we have previously described (Matsakas et al., 2012). Using this surgical protocol, left hindlimb is ischemic and the contralateral right hindlimb serves as the control. Tibialis anterior (TA) muscles were harvested at indicated time-point after the induction of ischemia and processed.

Laser Doppler blood flowmetry

Blood flow was measured in both the contralateral non-ischemic and ischemic TA from wild type and transgenic mice with a deep tissue laser Doppler flow probe (Vasamedics Laserflo BPM2). Blood perfusion in the ischemic hindlimb muscle is reported as the percent of perfusion in contralateral non-ischemic hindlimb muscle (ischemic/contralateral x100).

Immunohistochemistry

Serial transverse cryosections (9 μM thick at intervals of 80-100 μM) were obtained from the TA isolated from contralateral and ischemic hindlimbs of wild type and PGC1β transgenic mice. Frozen muscle sections were processed for CD31 immunohistochemical staining using a rat anti-mouse monoclonal antibody (AbD serotec; MCA2388) and visualized using suitable Alexa Fluor® secondary antibodies from Molecular Probes. Negative control staining by omitting either the primary or the secondary antibody was included in all sets of experiments. Immunostained sections were examined using a Zeiss Axioimager fluorescence microscope and images were captured using an Axiocam digital camera.

Serum creatine kinase (CK)

Tail vein blood was collected for 5-months old wild type and PGC1β transgenic mice and allowed to clot for 1 h and centrifuged at 13,000 rpm for 20 min. Serum was collected and stored at −80°C, and samples were assayed within 1 week from collection using a CK reagent set from Pointe Scientific, Inc. (Canton, MI, USA) according to the manufacturer's protocol.

Microfil perfusion and imaging

Whole-mount vascular imaging of the TA vasculature was performed using a 12% (w/v) microfil pigment solution of gouache in 4% PFA. The microfil solution was administered by intra-cardiac route in anesthetized mice, and the TA muscles were dissected, followed by serial dehydration in ethanol. Next, the tissues were incubated in fresh transparency solution that consisted of 1:1 benzylbezoate and benzylalcohol until tissues became transparent. After the muscles were processed, whole-mount tissue images were obtained on an inverted microscope (2 x magnifications).

Mitochondrial DNA isolation and quantification

Total DNA (genomic and mitochondrial) was prepared from gastrocnemius and quadriceps from WT and TG mice and digested with 100 µg/ml RNase A for 30 min at 37°C. The relative copy numbers of mitochondrial and nuclear genomes from 1 ng total DNA were determined by quantitative PCR (qPCR) with primers specific to mitochondrial *Cytb* (forward: 5′-CCTTCATACCTCAAAGCAACGA-3′; reverse: 5′-GATAAGTAGGTTGGCTACTAGGATTCAGT-3′) and nuclear *Rn18s* (forward: 5′-ACGGCCGGTACAGTGAAACT-3′; reverse: 5′-GAGCGAGCGACCAAAGGA-3′) genes. Serial dilutions of pooled DNA were analyzed in parallel to establish a standard curve.

Scratch migration assay

For migration assays, SVEC4-10 endothelial cells were cultures in DMEM (0.5% FBS) for 12 h followed by streaking at around 1 mm width with 1ml tip. After 24 h, the migrated cells beyond the edge were counted in 3 random fields (5 x magnification).

Succinate dehydrogenase (SDH) staining

SDH staining was performed on 9 mM cryo-sections of TA muscles from WT and muscle-specific PGC1β transgenic mice. Briefly, the muscle sections were incubated at 37°C for 30 min in substrate buffer [0.2M Phosphate buffer containing sodium succinate (250 mg/10ml) and NBT (20mg/10ml)]. Following incubation, sections were washed three times with water following by two washes each with increasing and decreasing concentrations of acetone (30%, 60%, 90%). Finally, the sections were washed three times with water and mounted in an aqueous mounting media and visualized under light microscope.

Microarray analysis

Genome wide gene expression analysis was performed on RNA isolated from TA muscles in WT and transgenic mice. Three hundred nanograms of total RNA (from each sample) was amplified and purified using Illumina TotalPrep RNA Amplification Kit (Ambion, IL1791), following the kit instructions. Briefly, first strand cDNA was synthesized by incubating RNA with T7 oligo(dT) primer and reverse transcriptase mix at 42 ºC for 2 h. RNase H and DNA polymerase master mix were immediately added into the reaction mix following reverse transcription and were incubated for 2 h at 16 ºC to synthesize second strand cDNA. RNA, primers, enzymes and salts that would inhibit

in vitro transcription were removed through cDNA filter cartridges (part of the amplification kit). In vitro transcription was performed and biotinylated cRNA was synthesized by 14 h amplification with dNTP mix containing biotin-dUTP and T7 RNA polymerase. Amplified cRNA was subsequently purified and concentration was measured by NanoDrop ND-1000 Spectrophotometer (NanoDrop Technologies, DE). An aliquot of 1.5 μg of amplified products were loaded on to Illumina Sentrix Beadchip Array Mouse WG-6.v2 arrays, hybridized at 58ºC in an Illumina Hybridization Oven (Illumina, Cat# 198361) for 17 h, washed and incubated with straptavidin-Cy3 to detect biotin-labeled cRNA on the arrays. Arrays were dried and scanned with BeadArray Reader (Illumina, CA). Data were analyzed using GenomeStudio software (Illumina, CA). Clustering and pathway analysis were performed with GenomeStudio and Ingenuity Pathway Analysis (Ingenuity Systems, Inc.) software, respectively.

Aortic capillary sprouting assay

As described previously (Sawada et al., 2009; Sawada et al., 2008), thoracic aorta segments (~1mm long, 8-10 segments per aorta) were dissected from 3-4 mice per group and implanted in 0.15 ml of 1% rat-tail collagen (BD Bioscience, San Jose, CA). For rescuing PGC1β expression in aortic rings from PGC1β-/- mice, we used PGC1β lentivirus particles. For this, 10-12 aortic rings from PGC1β-/- mice were incubated with 200 μl PGC1β lentivirus particles (titer >1X10^5) for 6 h in the presence of 5 μM/ml polybrene (Millipore) and implanted in 0.15ml of 1% rat tail collagen. Each explant was photographed under microscope at day 7. The *ex vivo* angiogenesis was determined as the area of capillary outgrowth using Image J software.

REFERENCES

Matsakas, A., Yadav, V., Lorca, S., Evans, R.M., and Narkar, V.A. (2012). Revascularization of ischemic skeletal muscle by estrogen-related receptor-gamma. Circulation research *110*, 1087-1096.

Sawada, N., Kim, H.H., Moskowitz, M.A., and Liao, J.K. (2009). Rac1 is a critical mediator of endothelium-derived neurotrophic activity. Science signaling *2*, ra10.

Sawada, N., Salomone, S., Kim, H.H., Kwiatkowski, D.J., and Liao, J.K. (2008). Regulation of endothelial nitric oxide synthase and postnatal angiogenesis by Rac1. Circulation research *103*, 360-368.